



## Review

## Selective C–H oxidation catalyzed by metalloporphyrins

Miquel Costas\*

Department de Química, Universitat de Girona, Campus de Montilivi, Girona 17071, Spain

## Contents

1. Introduction .....	2912
2. P450 as a model .....	2913
3. Catalytic C–H oxidation reactions: catalyst evolution .....	2913
4. Reaction mechanisms of C–H oxidation at P450 and synthetic models .....	2914
4.1. The rebound mechanism .....	2914
4.2. Two state reactivity scenarios .....	2916
4.3. Multiple oxidants scenarios .....	2918
4.3.1. Metal–oxidant adducts .....	2918
4.4. The role of the axial ligand .....	2919
4.5. Photochemical generation of Fe <sup>V</sup> –oxo species .....	2919
4.6. Agostic interactions .....	2920
4.7. The oxo–hydroxo tautomerism .....	2920
5. C–H oxidations at manganese porphyrins .....	2921
6. Selective oxidations at iron and manganese porphyrins .....	2922
6.1. Regioselective oxidations mediated by halide-substituted metalloporphyrins .....	2922
6.2. Shape dependent hydroxylations .....	2923
6.3. Regio and stereoselective hydroxylations with metalloporphyrins containing substrate recognition motifs .....	2923
6.4. Regio and stereoselective hydroxylations with metalloporphyrins without assistance of substrate recognition motifs .....	2925
7. C–H Oxidations catalyzed by ruthenium and osmium porphyrins .....	2925
8. Enantioselective C–H oxidations .....	2928
9. Summary and future prospects .....	2931
Acknowledgements .....	2931
References .....	2931

## ARTICLE INFO

## Article history:

Received 19 February 2011

Accepted 23 June 2011

Available online 6 July 2011

## Keywords:

Metalloporphyrin

C–H Oxidation

Reaction mechanisms

Selectivity

High-valent

Metal–oxo species

## ABSTRACT

Selective oxidation of saturated C–H bonds remains a challenge in modern chemistry. The inert nature of such bonds requires the use of highly reactive reagents, and this poses major challenges in terms of chemo, regio and stereoselectivity. Metalloporphyrins based in iron, manganese and ruthenium constitute a unique family of catalysts capable of generating these highly reactive, but at the same time highly selective oxidants, thus exquisitely mediating selective oxidations of C–H bonds. The mechanisms underlying these reactions are collected and discussed in the present work. Recent advances in the application of these catalysts in the oxidation of complex organic molecules are also reviewed.

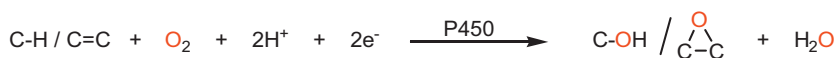
© 2011 Elsevier B.V. All rights reserved.

## 1. Introduction

Alkane oxidation reactions are of great technological interest because the abundance of hydrocarbons in nature, especially from natural gas and crude oil, makes them convenient chemical feedstocks, towards the production of oxygen-containing chemicals [1–4]. On the other hand, oxidized alkane frameworks are

\* Tel.: +34 972 419842; fax: +34 972 418150.

E-mail address: [miquel.costas@udg.edu](mailto:miquel.costas@udg.edu)



**Scheme 1.** Hydroxylation and epoxidation reactions catalyzed by cytochrome P450.

ubiquitous constituents of organic molecules with biological relevance. Methodologies for selective oxidation of alkane C–H bonds are very attractive because they can open novel straightforward synthetic strategies, and therefore offer the possibility to redesign synthetic organic chemistry [5–8].

The direct conversion of alkyl C–H into C–O bonds is a thermodynamically highly favorable transformation, but it faces very fundamental challenging problems related with the kinetically inert nature of C–H bonds [9]. In order to overcome this lack of reactivity problem, highly reactive-oxidizing reagents are needed, and this factor poses major challenges in the characteristics of chemo and regioselectivity of their reactions [6].

Metalloporphyrins containing iron, manganese or ruthenium constitute unique families of catalysts capable of generating these highly reactive, but at the same time highly selective oxidants, thus mediating highly selective oxidations of C–H bonds. Enzyme-like exquisitely selective C–H bond oxidations in complex organic molecules, affording products in synthetically useful yields have been accomplished with this family of synthetic catalysts. In addition, reaction mechanisms by which a C–H bond is hydroxylated by a metalloporphyrin have been extensively studied over the last decades. Indeed, studies on the reactions of metalloporphyrins provide excellent lessons to understand most C–H oxidation reactions mediated by transition metal complexes.

The purpose of this review is to provide an overview of the reaction mechanisms by which metalloporphyrins, especially these that contain Fe, Mn and Ru ions, mediate selective C–H oxidation reactions, and to discuss advances in the field towards the development of efficient and selective C–H oxidation catalysts. Because of that, we have focused our review in metalloporphyrin systems for which C–H bond oxidation does not take place via free-diffusing radical mechanisms. Despite of this constraint, the field appears very rich and we have had to make some selection in the works covered. We apologize if the reader feels that some important contribution has passed unnoticed to us.

## 2. P450 as a model

The oxidation of C–H bonds catalyzed by synthetic metalloporphyrins has been extensively studied during the last three decades [10–15]. Such studies are inspired by oxidation reactions taking place in living organisms catalyzed by heme proteins, and specially by cytochrome P450 (P450) [12,14–18]. P450 is a family of iron enzymes ubiquitous in life forms ranging from bacteria to humans [16–21]. They are monooxygenases that catalyze the oxidation of a wide variety of biological substrates by means of dioxygen activation. In this process, one of the oxygen atoms is introduced into the organic substrate, while the second oxygen atom is  $2\text{e}^-$  reduced and forms a water molecule (Scheme 1). Oxidation reactions mediated by P450s play a central role in biosynthesis, metabolism and detoxification of harmful substances. Most interestingly, specific P450s catalyze highly selective oxygenations of steroids and participate in prostaglandin biosynthesis [18]. Specific bacterial P450s have been genetically engineered for large-scale biotransformations [22].

The active site of P450-camphor is known in detail from several X-ray crystal structures [20,23,24]. It contains a single ferric heme (iron protoporphyrin IX, Scheme 2) coordinated to a cysteinate sulfur. The sixth iron coordination site is empty, or occupied by either a water or hydroxide ligand. At this site,  $\text{O}_2$  binding and activation takes place.

The P450 family is considered the paradigm for oxygen activation and hydrocarbon oxidation by an iron center. Studies with synthetic metalloporphyrins have helped in the understanding of oxidation reactions taking place at this enzyme, but at the same time have led to the development of efficient and selective C–H oxidation catalysts.

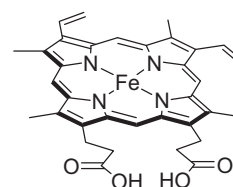
## 3. Catalytic C–H oxidation reactions: catalyst evolution

Development of porphyrin catalysts has evolved via successive generations [15]; Flat metalloporphyrins with no substituents at the meso positions were rapidly discarded because of very fast oxidative degradation [25]. This structural feature renders them very reactive towards meso cleavage via self-oxidation, to form a meso-hydroxyporphyrin derivative. Introduction of phenyl (and related) groups at the meso positions proved to be a key structural feature to ensure efficient catalytic oxidations by protecting these very reactive sites, and by providing steric protection that prevents the formation of catalytically inactive oxo-bridged dimers [15].

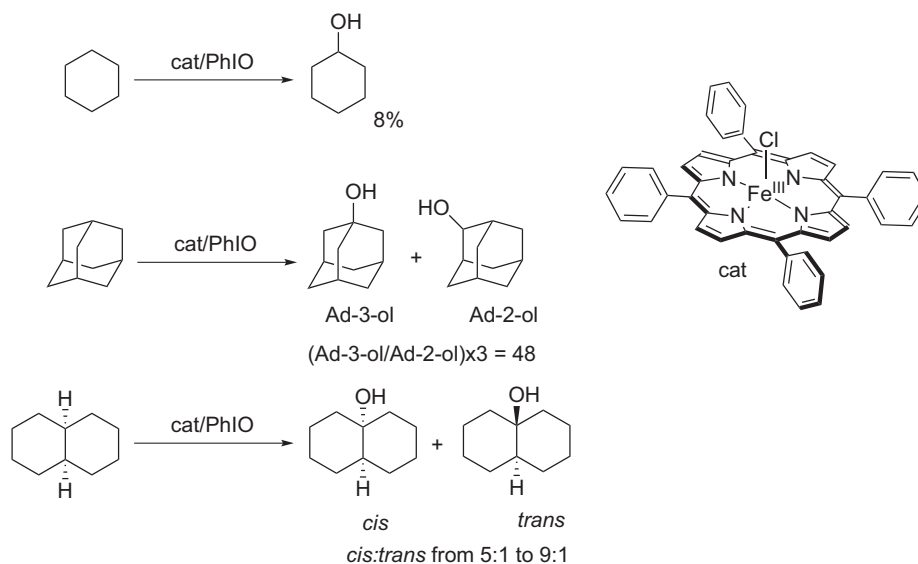
The first generation of successful catalysts in C–H oxidation reactions is formed by the different metal derivatives of the meso- $\alpha,\beta,\gamma,\delta$ -tetraphenylporphyrin (TPP) ligand. Iron, manganese and ruthenium are especially competent for catalytic oxidation reactions. The first synthetic system that closely reproduced the oxidation chemistry of P450 was described by Groves and co-workers. Chloro- $\alpha,\beta,\gamma,\delta$ -tetraphenylporphyrinatoiron(III) [ $\text{Fe}(\text{TPP})\text{Cl}$ ] utilizes iodosylbenzene ( $\text{PhIO}$ ) as oxidant to carry out the hydroxylation of alkanes (Scheme 3) [26,27]. Cyclohexane was hydroxylated to cyclohexanol in 8% yield, with little amount of cyclohexanone. Adamantane was oxidized to the corresponding adamantanol in 13% yield, with a high  $3^\circ/2^\circ$  C–H statistically corrected selectivity (48:1). Hydroxylation of *cis*-decalin occurs selectively at the tertiary C–H bonds affording 9-decanols with predominant retention of the configuration (*cis:trans* from 5:1 to 9:1).

The second generation of porphyrin catalysts is represented by meso-tetrakis(pentafluorophenyl)porphyrin TPFPP, [28] meso-tetramesitylporphyrin (TMP) [29,30], meso-tetrakis(2,6-difluororophenyl)porphyrin (TDFPP) and meso-tetrakis(2,6-dichlorophenyl)porphyrin (TDCPP) [31,32], and related ligands where alkyl or halogen groups have been introduced at *ortho*, *meta* and *para* positions of the phenyl rings attached to the macrocycle meso positions (Scheme 4). These ligands were designed with the aim of providing more efficient site isolation but also because the electron-withdrawing nature of the halide groups was envisioned to allow modulating the electrophilicity of the oxidant [15,33,34].

The third generation of catalysts (Scheme 4) builds on the previous idea by introducing halide atoms at the  $\beta$ -position of pyrroles, such as meso-tetrakis(2,6-dichlorophenyl)- $\beta$ -octabromoporphyrin,  $\text{Br}_8\text{TDCPP}$  [35], meso-tetrakis(2,6-



**Scheme 2.** Schematic diagram of iron protoporphyrin (heme).



**Scheme 3.** First example of a synthetic metalloporphyrin as catalyst for alkane hydroxylation reactions.

dichlorophenyl)- $\beta$ -octachloroporphyrin,  $\text{Cl}_8\text{TDCPP}$  [36], meso-tetramesityl- $\beta$ -octabromoporphyrin,  $\text{Br}_8\text{TMP}$  [37], meso-tetrakis(2,4,6-trimethyl-3-chlorophenyl)- $\beta$ -octachloroporphyrin,  $\text{Cl}_{12}\text{TMP}$  [38] and meso-tetrakis(pentafluorophenyl)- $\beta$ -octafluoroporphyrin,  $\text{F}_8\text{TPFPP}$  [39]. This large degree of halogenation in iron porphyrins causes large positive shifts in the iron(III)/(II) redox couple, protection of the porphyrin against oxidative damage, and severe saddling of the macrocyclic structure [40]. The latter structural feature favors monomeric porphyrin complexes with regard to formation of oxo-bridged dimers.

Further manipulation of the electronic properties of the porphyrin by introducing electron withdrawing nitro [41] or 4-(*N*-methylpyridinium) [42] groups has led to highly active species in hydroxylation reactions.

#### 4. Reaction mechanisms of C–H oxidation at P450 and synthetic models

##### 4.1. The rebound mechanism

The mechanism by which P450 hydroxylates a C–H bond has captivated chemists for years, and its study has provided fundamental knowledge that serves as a general paradigm for the C–H hydroxylation reaction [11,16–18,43]. The reaction bears very broad significance, which goes beyond the porphyrin field, and applies in some extent to almost any C–H oxidation reaction medi-

ated by a metal–oxo species. Because of that, its discussion in some detail is warranted.

Extensive studies in the reaction mechanism of P450, chloroperoxidases (CPO) and synthetic metalloporphyrins have led to the consensus that high valent metal–oxo species form from the interaction of the oxidant with the porphyrin metal site [17,20,42,44–49]. Oxo-iron(IV) porphyrin radical [ $\text{Fe}^{\text{IV}}(\text{O})(\text{Por}^{\bullet})$ ] species, known as Compound I (CpdI), have been spectroscopically characterized in the catalytic cycle of CPO, in synthetic iron porphyrins [46], and very recently in a P450 enzyme [44]. Despite a wide consensus exists on the latter formulation of CpdI, recent studies in laser flash photolysis of P450 mutants [50–53] and synthetic iron porphyrins [54] have shown formation of highly reactive intermediates formulated as oxo-iron(V) species, and that could be considered as an alternative formulation of CpdI.

The 1 e-reduced version of CpdI is known as CpdII. CpdII has been traditionally considered a poor oxidant, although recent work by Nam and co-workers in [ $\text{Fe}^{\text{IV}}(\text{O})(\text{Por})$ ] synthetic models suggests it may be a competent C–H oxidation agent [55,56].

The mechanism by which the P450 hydroxylates C–H bonds was initially proposed by Groves et al. [57], and it is known as the “Oxygen Rebound Mechanism”. The original proposal suggested that chemistry was taking place at a  $\text{Fe}^{\text{V}}=\text{O}$  species, but the current consensus is that the electronic structure of CpdI is best described as an oxo-iron(IV) porphyrin radical [ $\text{Fe}^{\text{IV}}(\text{O})(\text{Por}^{\bullet})$ ] [18]. The mechanism was subsequently extended to synthetic iron and manganese porphyrins, and in major or minor extent, it has proved to be of relevance to any C–H oxidation reaction mediated by a metal–oxo species. The mechanism involved rate determining hydrogen abstraction from the substrate ( $\text{R-H}$ ) by the terminally bound oxo ligand of the ferryl ( $\text{Fe}=\text{O}$ ) species, to form a caged alkyl radical and a [ $\text{Fe}^{\text{IV}}(\text{OH})(\text{Por})$ ] intermediate. In the second step, the hydroxide ligand is transferred to the alkyl radical (Scheme 5).

This mechanism accounts for the stereochemical, and allylic scrambling observed in the oxidation of norbornane [58], camphor [59] and cyclohexene [60] by P450 (Scheme 6). Synthetic metalloporphyrins have shown analogous results in the hydroxylation of norbornane [61] and cyclohexene [60]. Hydroxylation of exo-exo-exo-tetraduterionorbornane gave exo-alcohol with retention of the deuterium label, but with a significant amount of epimerization at the hydroxylated carbon center. On the other hand, hydroxylation of selectively tetraduterated cyclohexene occurs with substantial allylic scrambling. These observations provide

##### First Generation

$\text{R}_2 = \text{H}$ ,  $\text{R}_1 = \text{C}_6\text{H}_5$ ; TPP

##### Second Generation

$\text{R}_2 = \text{H}$ ,  $\text{R}_1 = \text{C}_6\text{F}_5$ ; TPFPP

$\text{R}_2 = \text{H}$ ,  $\text{R}_1 = 2,4,6\text{-Me}_3\text{-C}_6\text{H}_2$ ; TMP

$\text{R}_2 = \text{H}$ ,  $\text{R}_1 = 2,6\text{-Cl}_2\text{-C}_6\text{H}_3$ ; TDCPP

$\text{R}_2 = \text{H}$ ,  $\text{R}_1 = 2,6\text{-F}_2\text{-C}_6\text{H}_3$ ; TDFPP

##### Third Generation

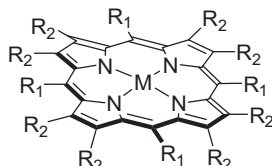
$\text{R}_2 = \text{Br}$ ,  $\text{R}_1 = 2,6\text{-Cl}_2\text{-C}_6\text{H}_3$ ;  $\text{Br}_8\text{TDCPP}$

$\text{R}_2 = \text{Cl}$ ,  $\text{R}_1 = 2,6\text{-Cl}_2\text{-C}_6\text{H}_3$ ;  $\text{Cl}_8\text{TDCPP}$

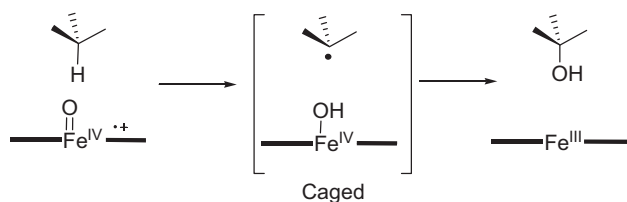
$\text{R}_2 = \text{Br}$ ,  $\text{R}_1 = 2,4,6\text{-Me}_3\text{-C}_6\text{H}_2$ ;  $\text{Br}_8\text{TMP}$

$\text{R}_2 = \text{Cl}$ ,  $\text{R}_1 = 2,4,6\text{-Me}_3\text{-C}_6\text{H}_2$ ;  $\text{Cl}_{12}\text{TMP}$

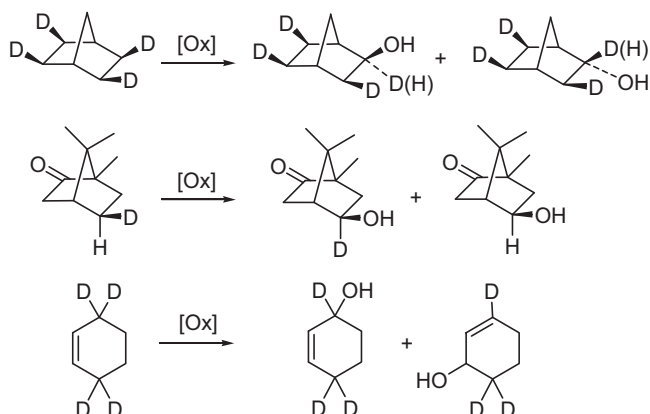
$\text{R}_2 = \text{F}$ ,  $\text{R}_1 = \text{C}_6\text{F}_5$ ;  $\text{F}_8\text{TPFPP}$



**Scheme 4.** Different generations of porphyrin catalysts.



**Scheme 5.** The rebound mechanism of P450 and iron porphyrins.



**Scheme 6.** Stereochemistry inversion in the oxidation of exo-exo-exo-tetradeuterionorbornane (top) and 5-exo-deuterated camphor (middle), and allylic scrambling observed in the oxidation of 2,2,5,5-tetradeuterated cyclohexene by P450 enzymes (bottom).

strong evidence for the formation of a short lived alkyl radical, which can undergo epimerization, or allylic rearrangement before recombination with the hydroxyl ligand takes place. On the other hand, the high, but not complete, retention of configuration also rules out the formation of freely diffusing radicals.

Primary kinetic isotope effects for the hydroxylation by P450 and synthetic iron porphyrins are usually large (4–22) [18,57,62]. These values are inconsistent with an insertion process but instead they indicate that breakage of the C–H bond is taking place in the rate determining step, strongly suggesting a non-concerted mechanism. Very large kinetic isotope effects, up to  $360 \pm 20$ , have been recently measured at  $-30^\circ\text{C}$  for the reaction of  $[\text{Fe}^{\text{IV}}(\text{O})(\text{TMP}^{\bullet})]$  with benzyl alcohol in acetonitrile, indicating that tunneling can be the major component of the reaction [63].

Radical lifetime can be estimated from the use of radical-clock substrates [64]. Radical clocks are molecules, which generally contain a cyclopropane ring, and that once converted into a radical,

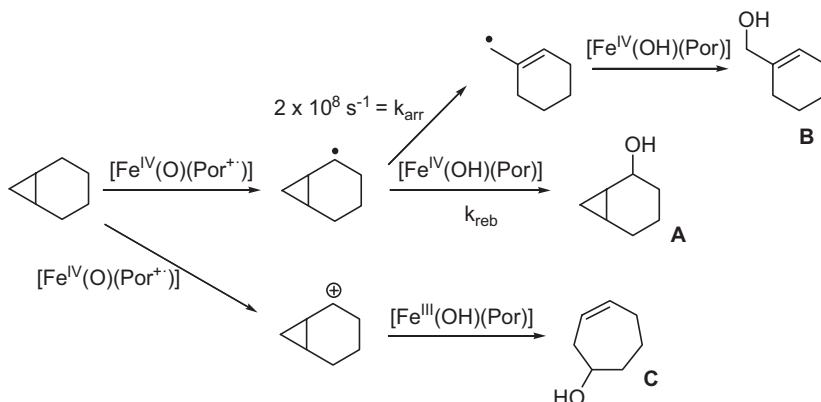
by means of a H-abstraction reaction, can either react with the reagent to generate a non radical product **A** ( $k_{\text{reb}}$  in Scheme 7), or in a competitive reaction they can undergo structural rearrangements involving cyclopropane ring opening, at a known rate ( $k_{\text{arr}}$ ) to generate a second radical that in turn reacts with the reagent to generate a rearranged non radical product **B**. Since  $k_{\text{arr}}$  is known, analysis of the **A/B** ratio allows to estimate the rate of the reaction that traps the non-rearranged radical ( $k_{\text{reb}}$ ). This scenario is illustrated in Scheme 7 for which norcaradiene is used as radical clock substrate. This particular substrate also allows investigation in the formation of cationic type of intermediates, which should lead to formation of rearranged product **C**. In the particular case of P450, alcohol **C** is not observed in the oxidation of norcaradiene [65].

A number of radical clock substrates have been used, leading to two different scenarios [18,66]. Radical clocks where the cyclopropyl ring is not directly attached to an aromatic ring consistently provide rebound rates between  $10^{10}$  and  $10^{11} \text{ s}^{-1}$  [64,65,67–70]. A second situation is observed in molecules where an aromatic ring is properly positioned to stabilize the rearranged radical. Because of this feature, these radical clocks have very fast rearrangement rates. Unexpectedly, using these substrates, rebound rates that reach up to  $1.4 \times 10^{13} \text{ s}^{-1}$  were determined (Scheme 8) [66,71,72].

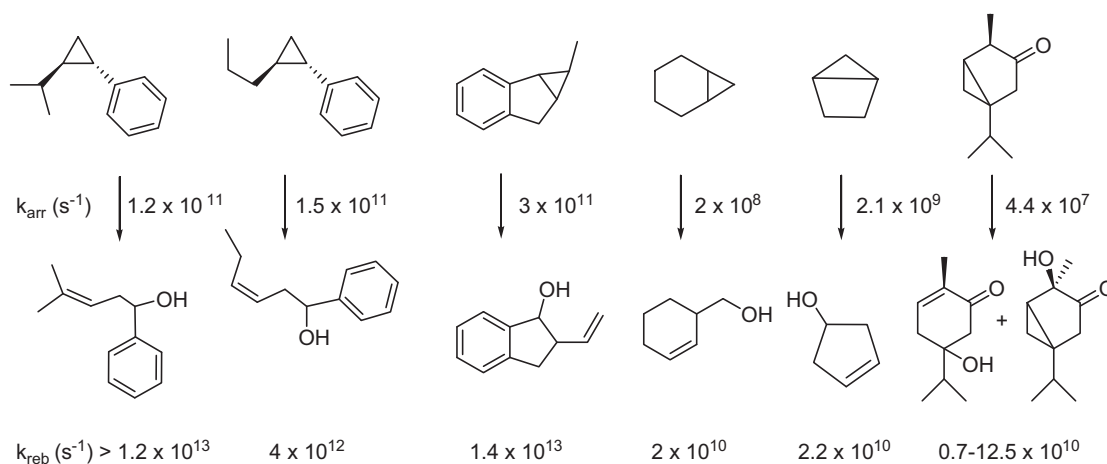
Newcomb et al. have reasoned that the extremely short lifetime ( $<100 \text{ fs}$ ) of the radical intermediates derived from specific radical-clock substrates is inconsistent with a real radical intermediate [73,74], and it is indeed comparable with the lifetime of a molecular vibration. Despite the concerted nature of the hydroxylation reaction, the short but finite lifetime of the radical indicates that nuclear motion is nonsynchronous (Scheme 9); abstraction of the hydrogen atom from the carbon must precede the formation of the C–O bond. For this to take place, a side-on approach of the oxygen atom to the substrate C–H bond would be required, so that the oxygen atom is within bonding distance to carbon at the moment of hydrogen atom abstraction.

On the other hand, the disparate values of rebound rates obtained from radical clock substrates have led to different theories, and constitute a field of controversy. On a very positive side, this debate has very much improved our understanding of the hydroxylation reaction.

- (a) The possibility that steric-structural constraints imposed by the active site could modulate the mobility of the radical was initially discarded because the two enantiomers of chiral radical probes, that are expected to interact differently within the chiral active site of the P450 enzyme, provide comparable rebound rates [75]. Also, rebound rates appear not to be correlated with radical-clock size.



**Scheme 7.** Different paths for the oxidation of the radical clock norcaradiene.



**Scheme 8.** Radical clocks, calibrated radical rearrangement rates ( $k_{arr}$ ), and rebound rates ( $k_{reb}$ ) derived from the experiments [18].

These conclusions should be reconsidered on the basis of experiments with chiral synthetic porphyrins. A very illustrative and elegant example of the impact of the 3D spatial structure of the oxidant-substrate supercomplex in the radical lifetime was provided by Groves et al. by showing that the relative stereochemistry of the substrate and porphyrin active site determines different stereochemical scrambling in the substrate [76,77]. Hydroxylation of deuterated chiral *d*<sub>1</sub>-ethylbenzene (Scheme 10) is catalyzed by chiral binaphthyl containing Fe-porphyrins [Fe(<sup>\*</sup>Por)Cl] affording 70% ee sec-phenethyl alcohol. The pro-*R*-hydrogen(deuterium) of ethylbenzene was hydroxylated with almost complete stereochemical retention at the hydroxylated carbon (23% **R<sub>H</sub>** over 1% **S<sub>H</sub>** for hydroxylation of (*R*)-*d*<sub>1</sub>-ethylbenzene, and 87% **R<sub>D</sub>** over 5% **S<sub>D</sub>** for hydroxylation of (*S*)-*d*<sub>1</sub>-ethylbenzene). Instead, pro-*S*-hydrogen(deuterium) atom of ethylbenzene atom underwent significant racemization (57% **S<sub>D</sub>** over 19% **R<sub>D</sub>** for hydroxylation of (*R*)-*d*<sub>1</sub>-ethylbenzene, and 6% **S<sub>H</sub>** over 2% **R<sub>H</sub>** for hydroxylation of (*S*)-*d*<sub>1</sub>-ethylbenzene). The partition between retention and inversion was nearly the same for the oxidation of the two enantiomers of *d*<sub>1</sub>-ethylbenzene (compare 23%/1% **R<sub>H</sub>**/**S<sub>H</sub>** with 57%/19% **R<sub>D</sub>**/**S<sub>D</sub>**, and also 57%/19% **S<sub>D</sub>**/**R<sub>D</sub>** with 6%/2% **S<sub>H</sub>**/**R<sub>H</sub>**), suggesting similar mobility of the radical intermediate at the active site. These results indicate that the rate of epimerization is dependent on the fit and mobility of the substrate at the active site.

- (b) Newcomb, Hollenberg and co-workers proposed that the discrepancies in the radical rebound rate could be due to a com-

petition between an ionic and a radical mechanism [66,78]. In the ionic mechanism, carbocationic intermediates are formed, and rearrange with the same skeletal reorganization as the corresponding radicals, but at different, unknown rates. Cation derived products have indeed been detected in oxidations of substrate probes that could differentiate between cationic and radical paths [79], by P450 isozymes, albeit at low overall percentages (Scheme 11) [74,78].

The same authors have also suggested that the determined slow rebound rates ( $<10^{11} s^{-1}$ ) might have resulted from a greater involvement of the carbocationic mechanism. However, since many of the radical clocks tested yielded exclusive unrearranged products, obligatory carbocation formation is excluded.

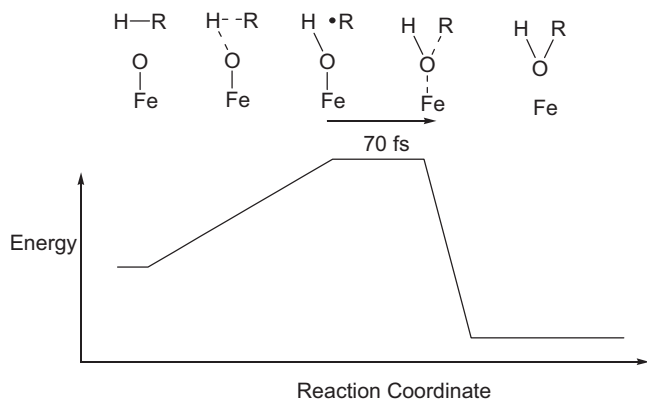
Two different mechanistic scenarios have been proposed to account for the formation of cationic intermediates (Scheme 12):

Path a) involves initial hydrogen atom transfer to the oxo-iron unit, rapidly followed by fast electron transfer (ET).

A second possibility (path b) is that O<sub>2</sub>-activation at P450 results in the formation of highly electrophilic HO<sup>+</sup> species via heterolytic O–O bond cleavage of the Fe<sup>III</sup>–O–OH P450 species. The HO<sup>+</sup> species inserts then into the C–H bond of the substrate (R–H), and the resulting [R–OH<sub>2</sub>]<sup>+</sup> species can lose a H<sup>+</sup> to yield the unrearranged alcohol (R–OH), or lose a water molecule, forming a carbocationic species (R<sup>+</sup>). Formation of HO<sup>+</sup> species via a “sommersault” mechanism has been computationally validated by Bach and Dimitrenko [80]. However, this proposal (Scheme 12 bottom) differs from the common observation that heterolytic cleavage of [Fe<sup>III</sup>(O–OH)(Por)] species commonly result in formation of high valent iron-oxo species.

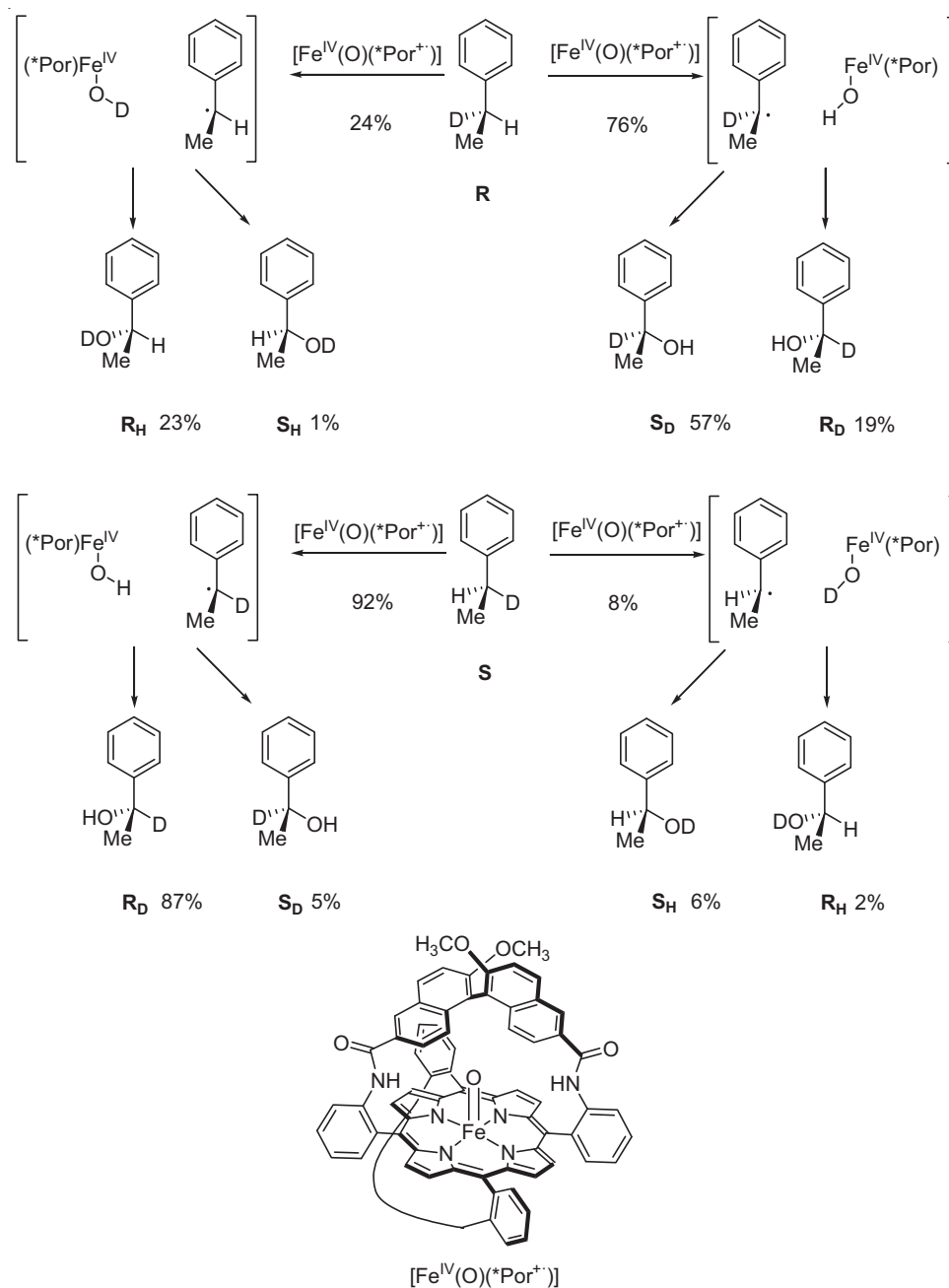
#### 4.2. Two state reactivity scenarios

According to a theoretical model developed by Shaik et al., the apparent disparate values on the rates of rebound reflect the fact that reactions between Cpdl and alkanes occur in a multistate spin scenario [81–83]. Shaik et al. proposed a two state reactivity (TSR) scenario for the reaction of Cpdl with methane (as a prototypical substrate) [84,85]. Computations estimated that Cpdl has two nearly isoenergetic spin configurations depending on whether the porphyrin radical cation is antiferromagnetically or ferromagnetically coupled respectively with the triplet ferric center. Both states react with the C–H bond via a similar transition state, with a linear O–H–C arrangement. Following the H-abstraction mechanism, a carbon centered radical is formed for both the low spin

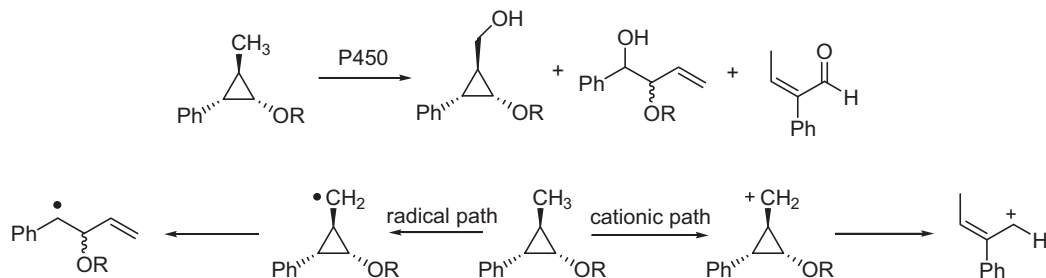


**Scheme 9.** Nonsynchronous concerted mechanism for P450 catalyzed hydroxylation.



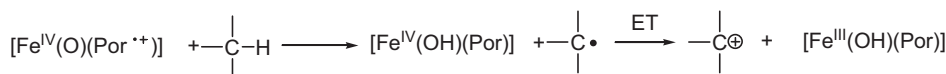


**Scheme 10.** Hydroxylation of deuterated chiral  $d_1$ -ethylbenzene catalyzed by chiral binaphthyl containing Fe-porphyrin  $[\text{Fe}(*\text{Por})\text{Cl}]$  [76].

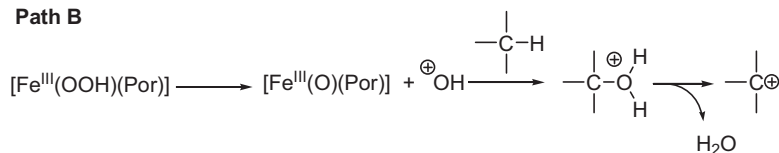


**Scheme 11.** Radical vs. cationic paths in radical clock substrates. (Top) Products produced from cytochrome P450 oxidations of second-generation hypersensitive probes. (Bottom) Concept of second-generation hypersensitive probes; production of a cyclopropylcarbinyl radical results in ring opening to a benzylic radical product, whereas formation of a cyclopropylcarbinyl cation leads to fragmentation favoring an oxonium ion.

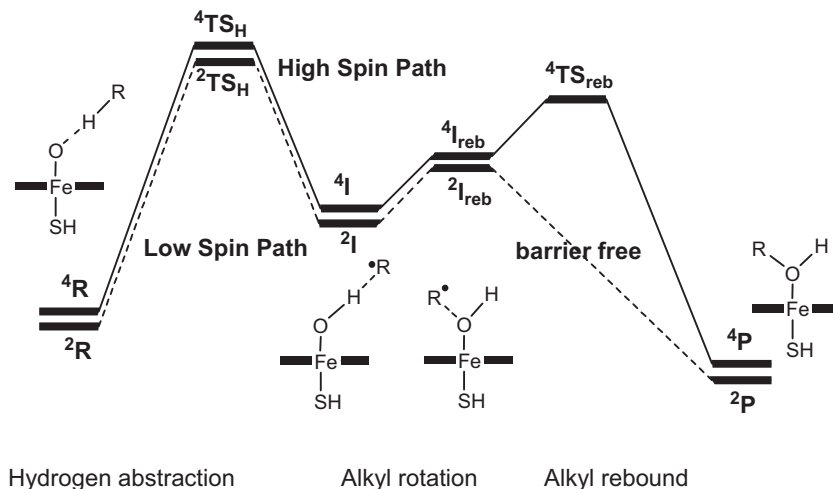
## Path A



## Path B



**Scheme 12.** Mechanistic paths for the formation of carbocationic intermediates in the reaction mechanism of P450.



**Scheme 13.** Generic transition state reactivity (TSR) in P450 hydroxylation reactions.

Source: Taken and adapted from Ref. [82].

and the high spin trajectories. At this point, an important difference arises. The barrier for the rebound process involving collapse of the carbon centered radical with the  $\text{Fe}^{\text{IV}}(\text{O})$  center leading to C–O bond formation in the high spin state is considerable, which implies that the radical has a significant lifetime. On the other hand, rebound at the low spin state occurs via a very small barrier. This scenario provides a reasonable explanation for the somewhat substrate dependent rebound rate. The two paths are very close in energy and thus it is very likely that the nature of the substrate impacts on the relative population of the two states (Scheme 13).

High level computations have shown that once formed, the carbon centered radical is susceptible to undergo weak, yet significant interactions with different residues at the active site and/or with the  $\text{Fe}^{\text{IV}}\text{--OH}$  unit, and these interactions may impact in the lifetime of the radical [86,87]. Spatial structure of the active site and the constraint imposed in the substrate and/or radical mobility can also affect the radical lifetime. Furthermore, a substrate C–H bond of high energy can require tight encounter between the  $\text{Fe}=\text{O}$  unit and the C–H bond. That will facilitate the fast reaction between the radical and the  $\text{Fe}\text{--OH}$ . Finally, competitive contributions between tunneling and over-the-barrier reactions can also have an impact on radical lifetime.

A very important consequence of the TSR scenario is that it offers a satisfactory rationale for apparently contradicting observations. Furthermore, this theory also accounts for a single oxidant (CpdI) to exhibit a rather “chameleonic” nature susceptible to be understood as a multiple oxidant scenario (*vide infra*) [84,85,88–92].

### 4.3. Multiple oxidants scenarios

#### 4.3.1. Metal–oxidant adducts

Several experimental evidences suggest that additional oxidants to the ferryl species  $[\text{Fe}^{\text{IV}}(\text{O})(\text{Por}^{\bullet+})]$  can be also competent for mediating C–H oxidation reactions in P450 and model systems [43,62,93–96].

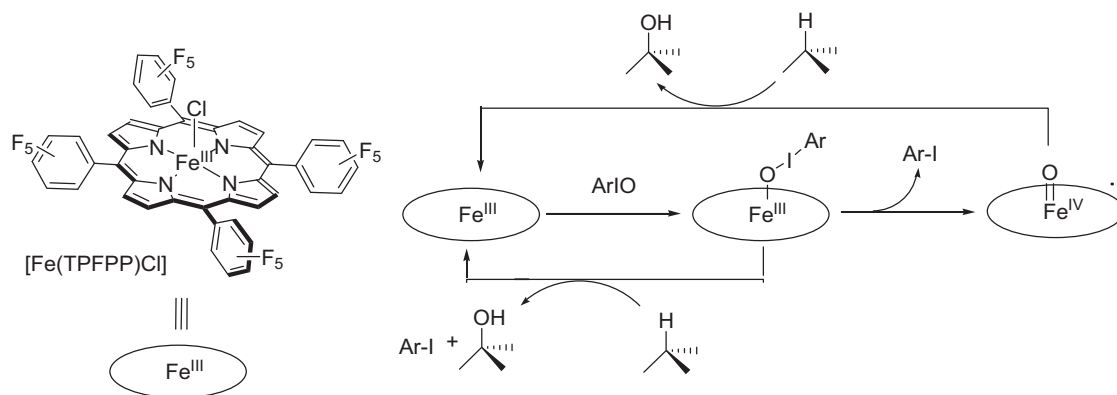
Collman, Brauman and co-workers studied the competitive oxidation of alkane substrates with various iodosylarenes, using  $[\text{Fe}(\text{TPFP})\text{Cl}]$  (Scheme 14) as catalyst. Relative ratios of oxidized products, understood as relative substrate reaction rates, were found dependent on the nature of the oxidant (Table 1). This is an indication that the active species responsible for the C–H oxidation activity, generated from different terminal oxidants, is

**Table 1**  
Competitive oxidation of alkanes with different oxidants catalyzed by  $[\text{Fe}(\text{TPFP})\text{Cl}]$ .

Substrate 1	Substrate 2	$k_1/k_2^a$		
		PhIO	F5-PhIO	IBDA <sup>b</sup>
c-Heptane	c-Hexane	2.4(2)	1.6(2)	
c-Heptane	c-Pentane	5.9(2)	4.9(2)	
c-Heptane	$d_{12}$ -c-Hexane	13(1)		10(1)
c-Hexane	c-Pentane	2.5(1)	3.1(1)	2.2(1)
c-Hexane	$d_{12}$ -c-Hexane	5.8(2)	4.3(2)	6.3(2)
c-Pentane	$d_{12}$ -c-Hexane	2.3(1)		2.8(2)
c-Hexane	n-Pentane	5.2(3)	4.1(3)	

<sup>a</sup> Numbers in parenthesis indicate the error (95% confidence level) in the final digit.

<sup>b</sup> IBDA, iodobenzene diacetate.



**Scheme 14.** Multiple oxidant scenario mechanistic proposal of Collman, Brauman, et al.

not the same in all cases. The dependence between the selectivity of the reactions on the nature of the oxygen-atom donor led the authors to conclude that the latter is involved in the rate-determining step. It was therefore proposed that besides the high valent  $[\text{Fe}^{\text{IV}}(\text{O})(\text{Por}^{+\bullet})]$  species, a complex formed by the oxidant and the porphyrin  $[\text{Fe}^{\text{III}}(\text{O}(\text{Ar})(\text{Por}))]$ , that precedes the formation of the ferryl species, can also be by itself a C–H oxidation agent [95].

Interestingly a similar conclusion was reached by Meunier et al. after studying the K.I.E. arising from the intramolecular competition in the hydroxylation of 1,3-deuteroadamantane catalyzed by iron and manganese porphyrins with different oxidants (*vide infra*) [62].

An alternative interpretation of the role of PhIO in C–H oxidations mediated by P450 was provided by Shaik et al on the basis of DFT computations, within the frame of the multiple-state scenario. The authors proposed that in the native enzyme route, the reaction proceeds via the doublet spin state of CpdI and leads to a low KIE value. PhIO, however, diverts the reaction to the quartet spin state of CpdI, which leads to higher KIE values [97].

Reversible reaction between  $[\text{Fe}^{\text{IV}}(\text{O})(\text{Por}^{+\bullet})]$  and iodoaromatic moieties to form  $[\text{Fe}^{\text{III}}(\text{O}(\text{Ar})(\text{Por}))]$  species ( $\text{Por} = \text{TDCPP}$  and  $\text{TDFPP}$ ) has also been proposed by Nam et al. to account for differences in isotopic labeling experiments in epoxidation reactions [98,99]. The extend of the equilibrium is dependent in the nature of the aromatic ring Ar, and the electronic nature of the porphyrin.

Along a similar track, Nam et al. studied the hydroxylation of alkanes with MCPBA catalyzed by  $[\text{Fe}(\text{TPFPP})(\text{X})]$  ( $\text{X} = \text{CF}_3\text{SO}_3$ , OH and Cl) and concluded the implication of a second electrophilic C–H oxidant besides the ferryl species [94]. Reaction of MCPBA with  $[\text{Fe}(\text{TPFPP})\text{Cl}]$  in a solvent mixture of  $\text{CH}_2\text{Cl}_2$  and  $\text{CH}_3\text{CN}$  at  $-40^\circ\text{C}$  results in the formation of  $[\text{Fe}^{\text{IV}}(\text{O})(\text{TPFPP})]$ , presumably formed via homolytic cleavage of the O–O bond of  $[\text{Fe}^{\text{III}}(\text{OOC}(\text{O})\text{Ar})(\text{TPFPP})\text{Cl}]$  (Scheme 15). When an alkane was present, formation of  $[\text{Fe}^{\text{IV}}(\text{O})(\text{TPFPP})]$  was inhibited, and the corresponding alcohol was obtained as product. The latter hydroxylation is stereospecific, as no scrambling was observed when *cis*-1,2-dimethylcyclohexane (*cis*-1,2-DMCH) was employed as substrate. The degree of inhibition was dependent on the strength of the C–H bond. Instead, reaction of  $[\text{Fe}(\text{TPFPP})(\text{CF}_3\text{SO}_3)]$  with MCPBA results in formation of  $[\text{Fe}^{\text{IV}}(\text{O})(\text{TPFPP}^{+\bullet})(\text{CF}_3\text{SO}_3)]$ . The reaction was not inhibited by the presence of substrate, but the latter ferryl species does react with the alkane.

It was then proposed that the  $[\text{Fe}^{\text{III}}(\text{OOC}(\text{O})\text{Ar})(\text{TPFPP})\text{Cl}]$  species is an electrophilic oxidant capable of mediating stereospecific C–H hydroxylation, and that this reaction is in competition with the homolysis path. Instead,  $[\text{Fe}^{\text{III}}(\text{OOC}(\text{O})\text{Ar})(\text{TPFPP})(\text{CF}_3\text{SO}_3)]$  undergoes very fast O–O heterolytic cleavage before reaction with the substrate can take place, and in this case, the ferryl

$[\text{Fe}^{\text{IV}}(\text{O})(\text{CF}_3\text{SO}_3)(\text{TPFPP}^{+\bullet})]$  intermediate is responsible for C–H hydroxylation. Isotopic labeling experiments, by performing oxidation reactions in the presence of  $\text{H}_2^{18}\text{O}$ , constitute a very informative mechanistic tool to further address this scenario. Water exchange can occur at  $\text{Fe}=\text{O}$  units by means of an oxo-hydroxo tautomerism (*vide infra*) [100,101]. Instead,  $[\text{Fe}^{\text{III}}-\text{OOR}(\text{Por})]$  ( $\text{R} = \text{H}$ , alkyl, aryl, acyl) species do not exchange the oxygen atoms with water. Consistent with this scenario, isotopic labeling experiments with  $\text{H}_2^{18}\text{O}$  indicated that reactions catalyzed by  $[\text{Fe}(\text{TPFPP})\text{Cl}]$  showed very little incorporation of  $^{18}\text{O}$  into products ( $4 \pm 1\%$ ). Instead, reaction catalyzed by  $[\text{Fe}(\text{TPFPP})(\text{CF}_3\text{SO}_3)]$  showed the same level of  $^{18}\text{O}$  incorporation ( $31\text{--}33 \pm 3\%$ ) as in the reactions where  $[\text{Fe}^{\text{IV}}(\text{O})(\text{TPFPP}^{+\bullet})]$  was previously generated *in situ* and used as oxidant. In conclusion, both  $[\text{Fe}^{\text{IV}}(\text{O})(\text{Por}^{+\bullet})]$  and  $[\text{Fe}^{\text{III}}(\text{OOC}(\text{O})\text{Ar})(\text{Por})(\text{X})]$  are proposed to be competent hydroxylating species, and the nature of the axial ligand appears to be somewhat crucial to regulate reactivity. It is not clear though its exact role. The proposed hydroxylating activity of  $[\text{Fe}^{\text{III}}(\text{OOC}(\text{O})\text{Ar})(\text{Por})\text{Cl}]$  species may result from an enhanced electrophilicity caused by the axial Cl atom, or alternatively, because of a comparatively higher barrier for O–O breakage, which extends the lifetime of this intermediate to the point where substrate oxidation and O–O lysis are competing reactions.

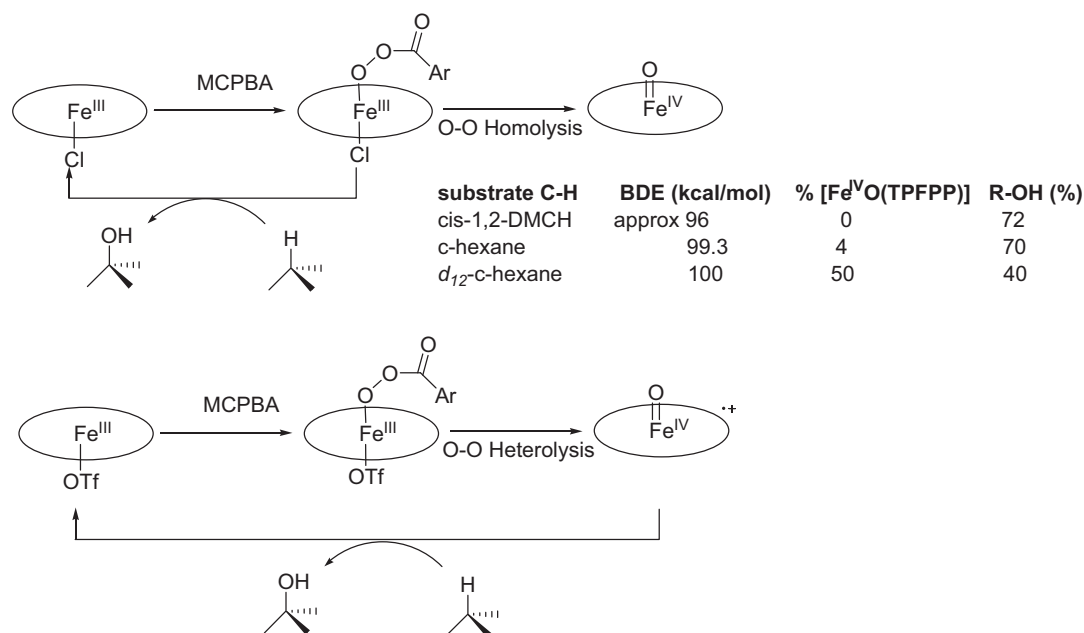
#### 4.4. The role of the axial ligand

The studies of Nam et al. reveal that the reactivity of synthetic metaloporphyrins can be dramatically dependent on the nature of the axial ligand [94,102–104]. Not only formation and stabilization of high valent metal-oxo species are affected by the nature of the axial ligand, but in addition, reaction mechanisms for the reaction of iron(IV)-oxo porphyrin radical intermediates with C–H bonds, as well as its selectivity are also influenced. The electron-donating ability of anionic axial ligands influences the activation energy for the C–H breaking step in the alkane hydroxylation reaction, and also the Fe–O bond distance of the iron-oxo species in the corresponding transition state. Iron(IV)-oxo porphyrin radical complexes bearing electron-donating axial ligands are more reactive in oxo-transfer and hydrogen-atom abstraction reactions. The reason is that as the ligand becomes a better electron donor, it strengthens the  $\text{FeO}-\text{H}$  bond and thereby enhances its H-abstraction activity. In addition, it weakens the  $\text{Fe}=\text{O}$  bond and encourages oxo-transfer reactivity [102,105].

#### 4.5. Photochemical generation of $\text{Fe}^{\text{V}}$ -oxo species

Newcomb and co-workers have shown that laser photolysis of iron(IV) porphyrin perchlorate complexes  $[\text{Fe}^{\text{IV}}(\text{TMP})(\text{OCIO}_3)_2]$



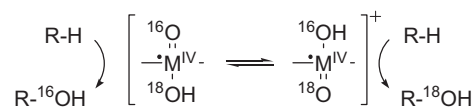


Scheme 15. Multiple oxidant scenario mechanistic proposal of Nam et al.

results in the formation of highly reactive transient species, [Fe<sup>V</sup>(O)(TMP)(OCIO<sub>3</sub>)] with unique spectroscopic features [106,107]. These new species react with organic substrates, including C–H oxidation reactions, with rate constants about five orders of magnitude faster than the iron(IV)–oxo radical cation analogue. In the absence of substrate, these Fe<sup>V</sup> species relax to a Cpdl-like species. The consequence of these observations is that transient highly reactive Fe<sup>V</sup>–oxo species could be also partially responsible for C–H oxidation reactions under catalytic conditions. Because of their high reactivity, under chemical catalytic conditions these species will remain undetected but they will be contributing to a multiple oxidant scenario.

#### 4.6. Agostic interactions

Collman et al. showed that cyclohexane hydroxylation by [Fe(TPFPP)Cl] and PhIO, as a model of cytochrome P-450, is inhibited by dihydrogen and methane [96]. The reaction rate for cyclohexanol formation decreases in the presence of H<sub>2</sub> and at P<sub>H<sub>2</sub></sub> = 1.4 atm, the value is half of the inhibited reaction rate. D<sub>2</sub> showed a slightly stronger inhibitory effect, while methane also showed inhibitory effect, though to a lesser extent than H<sub>2</sub>. Inhibition is reversible, and removing of the gas causes recovering of the initial rate. On the basis of these observations, the authors proposed a mechanism (Scheme 16) involving the reversible formation of a “σ-complex” between the substrate and the high-valent iron oxo center. Since agostic interactions of this kind increase the Brønsted acidity of the hydrogen, the authors propose that the second step of the reactions entails an intramolecular acid–base reaction. Because of this reaction, the C–H bond becomes polarized, prompting a proton to migrate to the basic oxo group, leaving the carbon bonded to the metal. This “insertion” would leave the oxidation state of the



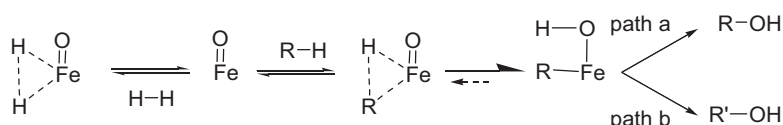
Scheme 17. Schematic diagram of the oxo–hydroxo tautomerism.

metal unchanged. Subsequent reductive elimination of the alkyl and hydroxyl groups would then lead to the hydroxylated product (path a, Scheme 16). For some alkyls, the reductive elimination could be preceded by rearrangement to form a more stable alkyl complex, resulting in products similar to those seen with carbon radicals or cations (path b, Scheme 16).

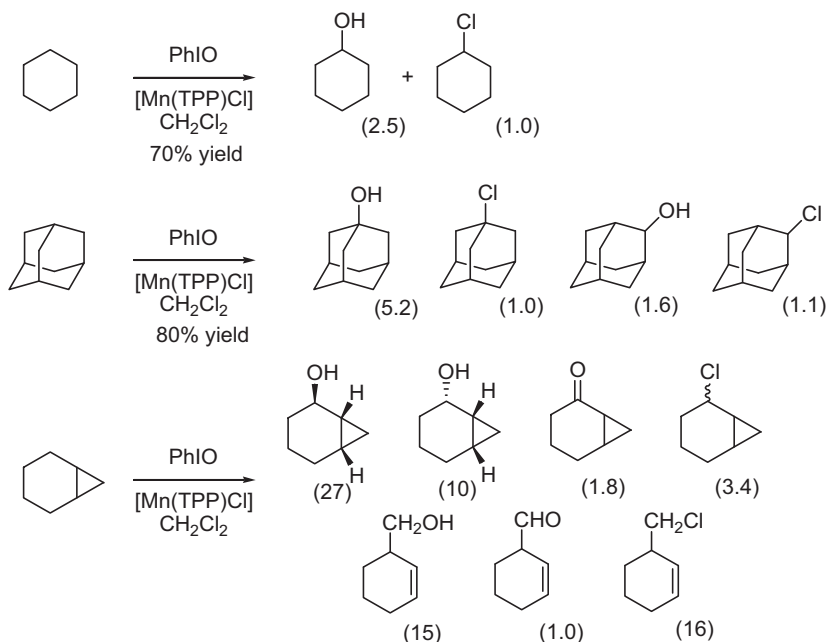
Groves et al. have pointed out that the effect of the gas on the relative reaction rates is relatively modest, and suggested that an alternative interpretation of these observations could be the existence of an interaction between H<sub>2</sub> and methane with the [Fe<sup>III</sup>(Por)] resting state, which is actually the most prevalent form of the catalyst inventory during turnover [77].

#### 4.7. The oxo–hydroxo tautomerism

This mechanism was most thoughtfully described for Mn-porphyrins [100,108] but it also applies to the iron analogues [101,109], and in general to any metal–oxo species. High valent metal–oxo porphyrin complexes can exchange the oxygen atom of the oxo ligand with water. This fact has been explained by the so-called oxo–hydroxo tautomerism, a mechanism involving a rapid shift of two electrons and one proton from a hydroxo ligand to the *trans* oxo group leading to the transformation of the hydroxo ligand into an electrophilic oxo entity on the opposite side of the initial oxo (Scheme 17) [100,108].



Scheme 16. Agostic mechanism for P450 and model systems.



**Scheme 18.** Catalytic oxidation of alkanes with  $[\text{Mn}(\text{TPP})\text{Cl}]$  and PhIO in  $\text{CH}_2\text{Cl}_2$ . Yields with respect to PhIO. Numbers in parenthesis correspond to relative amounts of reaction products [112].

As a result of this exchange, oxygen atoms that originate from water molecules can end up into oxidized products in metalloporphyrin catalyzed oxidations. The ‘oxo–hydroxo tautomerism’ has been used as mechanistic tool to characterize oxygen-atom transfer mechanisms mediated by metal–oxo species. That is based on the fact that neither autooxidation chains, nor reactions mediated by metal–peroxo species have a mechanism by which oxygen atoms from water could be incorporated into oxidized products. Therefore water incorporation into products can be understood as an indirect proof for the intermediacy of metal–oxo species in an oxidation reaction. This becomes important because the high reactivity of high-valent metal–oxo species usually precludes their direct observation. A cautious note at this point is needed because some oxidants like iodosylbenzene in the presence of transition metal complexes can undergo exchange of their oxygen-atom with water [110].

The oxo–hydroxo tautomerism is in competition with the bimolecular reaction between the metal–oxo species and the substrate (Scheme 17). Because of that, the level of water incorporation into products (easily monitored by running reactions in the presence of  $\text{H}_2^{18}\text{O}$ ) is inversely related to the reactivity of the substrate and to its relative concentration with respect to water [100,101]. The rate of the oxo–hydroxo tautomerism depends on the oxidation state, chemical nature of the metal–oxo species, and also on the presence of an available *trans* site to the oxo-ligand. Therefore, the lack of observation of water incorporation into products in a reaction does not imply that the reaction is not performed by a metal–oxo species, because the tautomerism may simply be slower than reaction with the substrate.

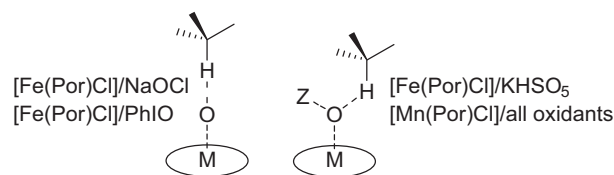
## 5. C–H oxidations at manganese porphyrins

Manganese porphyrins were early identified as efficient hydroxylation catalysts [111–114]. In pioneer work, it was described that  $[\text{Mn}(\text{TPP})\text{X}]$  ( $\text{X} = \text{Cl}, \text{Br}, \text{I}, \text{N}_3$ ) catalyze the oxidation of cyclohexane with PhIO as oxidant in benzene or  $\text{CH}_2\text{Cl}_2$  solvent to a mixture of cyclohexanol and cyclohexyl–X products (Scheme 18). In dibromomethane or bromotrichloromethane solvent, the corresponding alkyl bromides became the major products. Using PhIO/ $[\text{Mn}(\text{TPP})\text{X}]$


ratios between 0.5 and 9.5, combined product yields between 35 and 70% were obtained. Several pieces of evidence implicate the intermediacy of freely diffusing alkyl radicals in the reactions. Small amounts of radical derived products such as bicyclohexyl, and cyclohexylbenzene are obtained. Cyclohexyl–X products are also indicative of a ligand transfer reaction to the cyclohexyl radical, and halide extraction from the solvent.

Most significant, the oxidation of norcarane (Scheme 18) produces a mixture of products, including those that have undergone cyclopropyl ring opening. This constitutes a well-established radical rearrangement and it is indicative of a long-lived free-diffusing radical reaction [65]. The somewhat longer radical lifetime appears to be a fundamental difference from reactions catalyzed by the iron analogues [112]. An additional difference between Mn and Fe porphyrin catalyzed oxidations is that C–H KIE obtained with the former are substantially smaller than those measured with the later [62]. Evaluation of intramolecular KIE in the oxidation of 1,3-dideuterioadamantane by a series of iron and manganese porphyrins have led to the proposal that in Mn catalyzed oxidations the nature of the Mn–oxo intermediate is dependent on the nature of the oxidant. A bent transition state was proposed for Mn-catalyzed oxidations, where the oxo-delivering oxidant remains attached to the Mn–O unit (Scheme 19).

In the presence of selected additives such as imidazole [113], or ammonium acetate [114], Mn-porphyrins have been described as very active and efficient alkane oxidation catalysts, using  $\text{H}_2\text{O}_2$  as oxidant. Better yields with respect to analogous iron systems were obtained. The  $[\text{Mn}(\text{TDCPP})\text{Cl}]$  catalyst is particularly remark-



**Scheme 19.** Possible transition state geometries in hydroxylation reactions catalyzed by iron and manganese porphyrins ( $[\text{Fe}(\text{TMP})\text{Cl}]$ ,  $[\text{Mn}(\text{TMP})\text{Cl}]$ , and  $[\text{Mn}(\text{TDCPP})\text{Cl}]$ ) with ZO oxidants ( $\text{ZO} = \text{PhIO}, \text{NaOCl}, \text{KHSO}_5$ ).


  
 (800 equiv.)
 
 Oxidant (20 equiv.)  
 [Mn(TDCPP)Cl] (1 equiv)  
 Imidazole (10 equiv)  
 CH<sub>2</sub>Cl<sub>2</sub>:CH<sub>3</sub>CN 1:1  
 N<sub>2</sub>, RT, 2h

	Products <sup>a</sup>		(% regioisomers)	(-ol+one)
Oxidant	C-1	C-2	C-3	C-4
PhIO	4	65	27	3
H <sub>2</sub> O <sub>2</sub>	4	64	28	3

<sup>a</sup> Total yields, with respect to the oxidant, were 31% with PhIO and 11.5% with H<sub>2</sub>O<sub>2</sub>.

**Scheme 20.** Comparison between oxidants in the regioselective oxidation of heptane by [Mn(TDCPP)Cl].

able because it works under conditions where the alkane is not in large excess, but instead it is the limiting reagent. Good to excellent product yields (40–85%) were obtained by using 5 equiv. of H<sub>2</sub>O<sub>2</sub> and [Mn(TDCPP)Cl] (2.5 mol%) in the presence of imidazole (24 equiv.). On the other hand, in the absence of the base, only trace amounts of products were obtained.

The regioselectivity on the hydroxylation of *n*-heptane was the same, involving preferential hydroxylation of C-2, irrespective of the use of H<sub>2</sub>O<sub>2</sub>/imidazole, or PhIO as oxidant (Scheme 20). The site selective reactivity differs from a statistical regioisomeric distribution, and is indicative that a common metal-centered intermediate is responsible for the C–H oxidation event.

Oxo–Mn(V) species are proposed to be responsible for the oxidation activity. These highly unstable species have been spectroscopically characterized from the reaction of manganese porphyrins with various oxidants (H<sub>2</sub>O<sub>2</sub>, MCPBA, NaOCl, KHSO<sub>5</sub>) [30,115–120], and by laser flash photolysis of porphyrin–manganese(III) perchlorate complexes [106,121–123]. Combined spectroscopic methods indicate that they are best described as diamagnetic low-spin (*d*<sup>2</sup>, *S*=0) species. The description of the electronic structure of the porphyrin–manganese(V)–oxo species contrasts with that of the iron analogue, best described as oxoiron(IV) cation porphyrin radical [109].

However, experimental evidence about the ability of well-defined Mn<sup>V</sup>=O species to elicit C–H oxidation reactions is somewhat conflicting. Well-defined Mn<sup>V</sup>=O porphyrin [Mn<sup>V</sup>(O)(Por)], Por = TDCPP, TDFPP, TPFPP and TMP (Scheme 4) complexes were recently prepared and spectroscopically characterized [116]. The complexes proved kinetically competent for mediating O-atom transfer to phosphines and sulfides. However, no reaction with an alkane takes place under analogous conditions. Instead, further addition of PhIO oxidant elicits alkane oxidation products. These observations suggest that another yet uncharacterized species, generated from the reaction between Mn<sup>V</sup>=O and the oxidant may be responsible for the C–H oxidation.

On the other hand, the same [Mn<sup>V</sup>(O)(Por)] species react with hydride donor acridine type of substrates, via an initial proton coupled electron transfer, followed by rapid electron transfer [124]. Along the same track, water soluble Mn<sup>V</sup>–oxo and Mn<sup>IV</sup>–oxo porphyrin complexes [Mn<sup>V</sup>(O)<sub>2</sub>(tf<sub>4</sub>tmap)]<sup>3+</sup>, and [Mn<sup>IV</sup>(O)(OH)(tf<sub>4</sub>tmap)]<sup>3+</sup>, tf<sub>4</sub>tmap = meso-tetrakis(2,3,5,6-tetrafluoro-*N,N,N*-trimethyl-4-aniliniumyl)porphyrinato dianion, have been recently prepared and studied in the oxidation of alkylaromatics [115]. The complexes are proposed to react with these substrates through a hydrogen-atom abstraction mechanism, because reaction rates and C–H bond dissociation energies (BDE) have a linear correlation, and reactions exhibit large kinetic

isotope effects. As expected, the Mn<sup>IV</sup> species proved to be a milder oxidant than the Mn<sup>V</sup> counterpart, as evidenced by second order reaction rates differing two orders of magnitude. Photochemically generated Mn<sup>V</sup>–oxo species in acetonitrile solutions are also competent for mediating C–H oxidation reactions, and a small K.I.E. = 2.3 was estimated from the oxidation of ethylbenzene and its perdeuterated analogue [121]. The small value is consistent with an early transition state, indicative that the Mn<sup>V</sup>–oxo species are highly reactive.

## 6. Selective oxidations at iron and manganese porphyrins

The metal-centered nature of metalloporphyrin catalyzed C–H oxidations offers the possibility to develop regioselective and stereoselective C–H oxidation technologies. These represent very challenging transformations with scarce precedents in the synthetic literature, and because of that, they are especially valuable. Relevant contributions towards these goals have been collected in the following lines.

### 6.1. Regioselective oxidations mediated by halide-substituted metalloporphyrins

Halide substitution in the porphyrin affects both the efficiency and also the regioselectivity of metalloporphyrin catalyzed oxidation reactions (Table 2) [15,33,125]. In a comparative study in the hydroxylation of linear alkanes (pentane and heptane) catalyzed by porphyrins containing in their structure different halide substitution patterns, Mansuy and co-workers have shown that the total yields based on oxidant (PhIO) were very much dependent on the number of halogen substituents on the porphyrin ring (Table 2) [125]. Among the catalysts bearing no halogen substituent on their pyrrole rings, [Fe(TPP)Cl] and [Fe(TMP)Cl] provide low yield (4%), and only [Fe(TPFPP)Cl] provided a much better yield (70%).

The introduction of eight Cl or Br substituents on the pyrrole rings resulted in very efficient catalysts. [Fe(Cl<sub>8</sub>TDCPP)Cl] and [Fe(Br<sub>8</sub>TDCPP)Cl] afforded very remarkable yields up to 80% and 60% with respect to the oxidant in the oxidation of heptane and pentane, respectively.

In terms of regioselectivity, reactions occur predominantly at the methylene groups of the alkanes and oxidation at the methyl groups occurs in very little proportion (<2%). The regioselectivity of the reactions was also dependent on the nature of the catalyst. In most of the cases, regioselectivity reflects an almost statistical oxidation only linked to the number of secondary abstractable hydrogen atoms (40:40:20). However, in specific cases for catalysts [Fe(TMP)Cl], [Fe(TDCPP)Cl] and [Fe(Br<sub>6</sub>TDCPP)Cl] and where

**Table 2**Catalytic oxidation of heptane with porphyrin catalysts containing different halide substitutions.<sup>a</sup>

Catalyst	Product yields (%) <sup>b</sup>				Ketones	Yield (%)
	1-Heptanol	2-Heptanol	3-Heptanol	4-Heptanol		
[Fe(TDCPP)Cl]	1	14(58) <sup>c</sup>	7.5(30)	3.5(12)	6	38
[Fe(Br <sub>6</sub> TDCPP)Cl]	1.4	20(53)	12(32)	5.5(14)	2.5	44
[Fe(Br <sub>8</sub> TDCPP)Cl]	1.5	29.5(42)	28(41)	11(16)	5	80
[Fe(Cl <sub>8</sub> TDCPP)Cl]	1.5	29(43)	27(40)	10.5(16)	5	78
[Fe(TPFPP)Cl]	1	25.5(41)	24(39)	10.5(20)	4	69
[Fe(Cl <sub>8</sub> TPFPP)Cl]	1.5	22(41)	21.5(40)	9(19)	5	64
[Fe(TMP)Cl]	–	1.7(60)	0.8(31)	0.3(9)	0.5	4
[Fe(TPP)Cl]	–	1.2(38)	1.4(42)	0.6(20)	<0.2	3.5

<sup>a</sup> Catalyst/substrate/PhIO ratio 1/800/20 in CH<sub>2</sub>Cl<sub>2</sub>.<sup>b</sup> Product yields with respect to oxidant.<sup>c</sup> Values in parenthesis indicate relative ratio of alcohol with respect to the total amount of alcohols. Ketones also have the exact same ratio.

bulky Cl or methyl groups are attached at the ortho position of the meso-aryl substituents, higher regioselective oxidation of the more accessible C-2 carbon of heptane was observed. Further introduction of halide substituents on the pyrroles of the porphyrin led to a progressive change of this regioselectivity towards the statistical one. The same tendency was observed in pentane hydroxylation, a 78:22 C2:C3 ratio in oxidation products was obtained with [Fe(TDCPP)Cl], but a nearly statistic 67:33 ratio was obtained with [Fe(Cl<sub>8</sub>TDCPP)Cl].

## 6.2. Shape dependent hydroxylations

Manganese porphyrins with sterically protected pockets are shape-selective alkane hydroxylation catalysts (Table 3) [126,127]. With PhIO as oxidant, good regioselectivity was observed for the hydroxylation of linear alkanes at the less hindered methyl group by using the very sterically hindered (5,10,15,20-tetrakis(2',4',6'-

triphenylphenyl)-porphyrinato)manganese(III) acetate [Mn(TTPPP)(OAc)] as catalyst; the moderately hindered 5,10,15,20-tetrakis(2',4',6'-trimethoxyphenyl)porphyrinato)manganese(III) acetate shows little selectivity towards terminal C–H hydroxylation but does show enhancement for the adjacent, C-2 CH<sub>2</sub> site. Primary selectivity is dependent on the size and shape of the alkane substrate, with more bulky substituents giving greater primary selectivity.

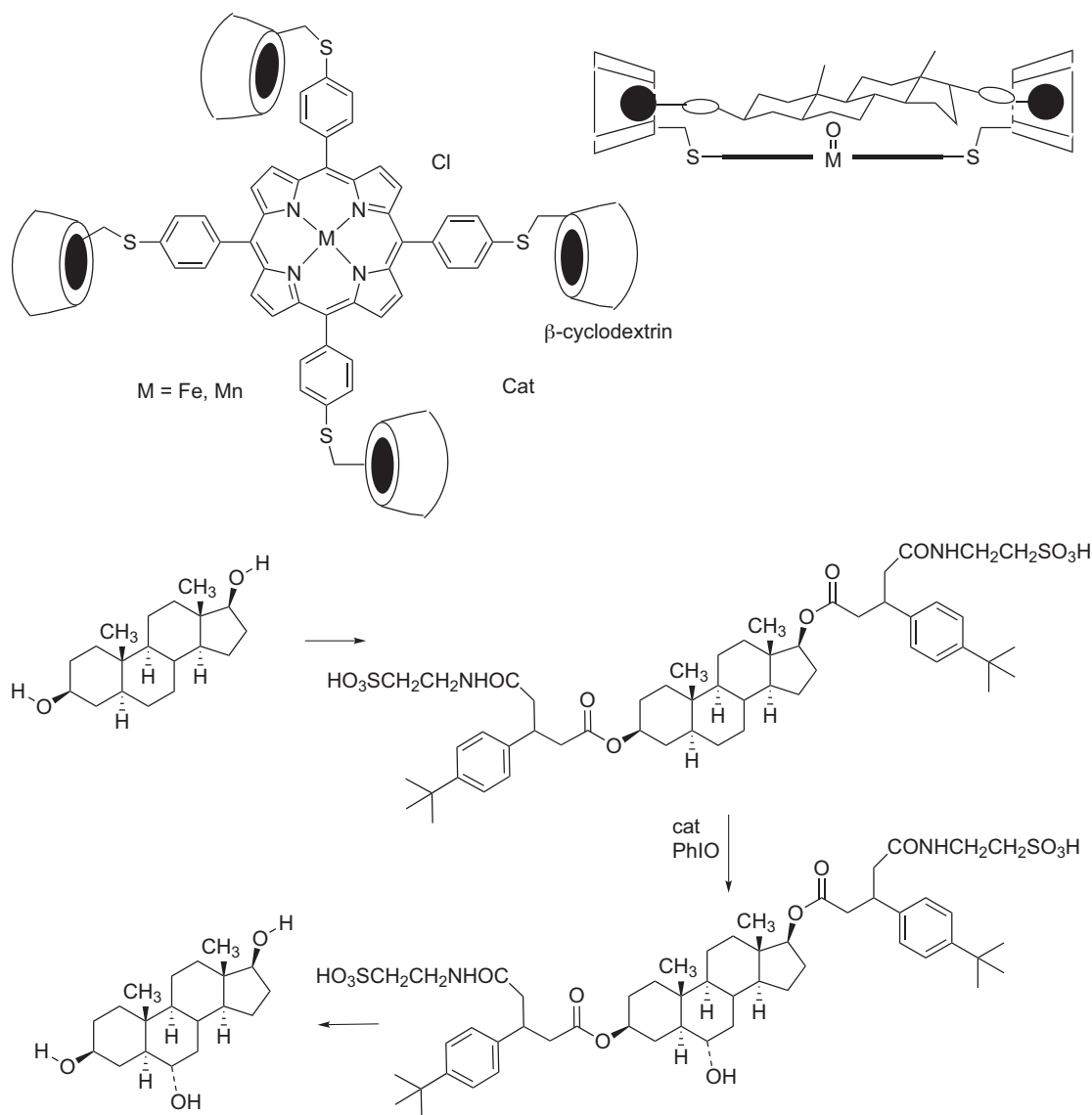
## 6.3. Regio and stereoselective hydroxylations with metalloporphyrins containing substrate recognition motifs

A very elegant strategy to attain regio and stereoselective hydroxylation of complex organic molecules has been developed by Breslow et al. by attaching substrate recognition sites to iron and manganese porphyrins [128–132]. This approach followed early work by Grieco and colleagues that showed intramolecular stoi-

**Table 3**Selectivity in the hydroxylation of *n*-alkanes with C<sub>6</sub>H<sub>5</sub>IO by Mn-porphyrins.

Substrate	Catalyst	Products (% yield)				Primary selectivity <sup>b</sup>
		1-ol	2-ol	3-ol	4-ol <sup>a</sup>	
<i>n</i> -C <sub>5</sub> H <sub>12</sub>	[Mn(TPP)(OAc)]	5	61	34	–	0.048
	[Mn(TTMP)(OAc)]	4	68	28	–	0.039
	[Mn(TTPPP)(OAc)]	10	75	15	–	0.11
<i>n</i> -C <sub>6</sub> H <sub>14</sub>	[Mn(TPP)(OAc)]	2	38	60	–	0.027
	[Mn(TTMP)(OAc)]	3	57	40	–	0.041
	[Mn(TTPPP)(OAc)]	19	62	18	–	0.31
<i>n</i> -C <sub>7</sub> H <sub>16</sub>	[Mn(TPP)(OAc)]	2	37	40	21	0.034
	[Mn(TTMP)(OAc)]	3	49	33	15	0.052
	[Mn(TTPPP)(OAc)]	26	52	17	5	0.59
<i>n</i> -C <sub>8</sub> H <sub>18</sub>	[Mn(TPP)(OAc)]	2	31	32	28	0.041
	[Mn(TTMP)(OAc)]	3	46	29	22	0.064
	[Mn(TTPPP)(OAc)]	21	48	16	15	0.53
<i>n</i> -C <sub>10</sub> H <sub>22</sub>	[Mn(TPP)(OAc)]	1	29	21	49	0.027
	[Mn(TTMP)(OAc)]	3	39	25	33	0.066
	[Mn(TTPPP)(OAc)]	18	43	13	26	0.58
<i>n</i> -C <sub>14</sub> H <sub>30</sub>	[Mn(TPP)(OAc)]	1	17	17	64	0.040
	[Mn(TTMP)(OAc)]	2	33	19	46	0.082
	[Mn(TTPPP)(OAc)]	17	37	15	31	0.82

<sup>a</sup> For *n*-decane, this also includes 5-decanol; for *n*-tetradecane, this also includes 5-tetradecanol, 6-tetradecanol and 7-tetradecanol.<sup>b</sup> The ratio of total primary alcohol to total secondary alcohols normalized for the relative number of hydrogen atoms.



**Scheme 21.** Regio and stereoselective hydroxylation of steroid substrates with  $\beta$ -cyclodextrin appended metalloporphyrin catalysts. Top left: catalyst structure. Top right: schematic diagram of the substrate oriented catalyst–substrate complex. Bottom: Substrate derivation with  $\beta$ -cyclodextrin binding groups, catalytic hydroxylation and substrate deprotection.

chiometric selective hydroxylation of steroids covalently attached to metalloporphyrin [133], or Mn-salen complexes [134]. In Breslow's approach, substrate binding sites can reversibly interact with the substrate, allowing for multiple turnover reactions. The geometric structure of the catalyst–substrate complex causes exquisite orientation of specific C–H bonds towards the catalytic site. This allows to override intrinsic C–H relative reactivity among different sites in catalytic hydroxylation reactions. In particular, selective hydroxylation of methylene in front of tertiary C–H bonds could be targeted. By following this strategy, catalytic regio and stereoselective hydroxylation of steroids is accomplished.

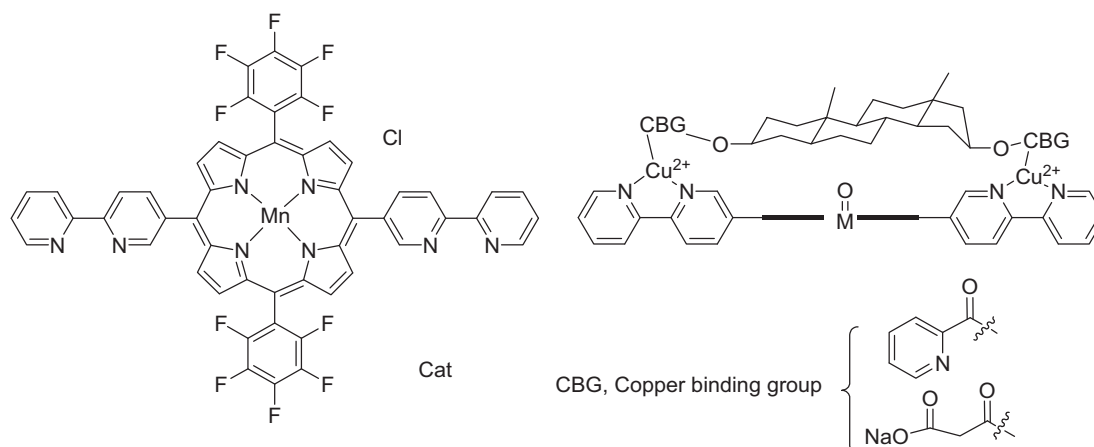
Two types of substrate binding sites have been developed so far (Schemes 21 and 22). The first and most thoughtfully developed approach involved the attachment of 2 or 4  $\beta$ -cyclodextrin substrate-binding sites at the meso positions of the metalloporphyrin. Selective hydroxylation at C-6 [128,129] and C-9 position of steroids [130,131] was performed (Scheme 21).

A second approach involves the attachment of 2,2'-bipyridyl groups at the porphyrin meso positions. Bipyridyl groups were introduced as  $\text{Cu}^{2+}$  ion binding sites. Steroid substrates derivatized with  $\text{Cu}^{2+}$  binding groups (CBG, acetylpyridine or phosphonoacetyl

groups, Scheme 23) were expected to interact with the  $\text{Cu}^{2+}$ -Porphyrin catalyst, thus specifically orienting the substrate with respect to the Mn active site.

Through this strategy, it was envisioned that the metal-ion coordination properties could offer a better control of the substrate–catalyst structure when compared with the ill-defined nature of hydrophobic interactions obtained with previously described cyclodextrins. Initial experiments involved introduction of four bipyridyl units in the metalloporphyrin catalyst. That resulted in fast catalyst degradation during oxidation reactions, presumably because of fast oxidation of pyridyl-nitrogen atoms [135]. To overcome this problem, two pentafluorophenyl groups, in relative *trans*-fashion, were introduced to improve catalyst stability, and in addition, to ensure that substrate interaction occurs with two bipyridine groups in *trans* relative position, thus offering a better control of the substrate–catalyst relative space orientation [132]. These modifications proved particularly successful and in the presence of  $\text{Cu}^{2+}$  ions, acting as coordinating linkers, steroid substrates containing Cu-binding units are hydroxylated with good regioselectivity and turnover numbers up to 32 (Scheme 23).





**Scheme 22.** Left: Bipyridyl substituted manganese porphyrin catalysts. Right: Schematic diagram of the interaction between catalyst,  $\text{Cu}^{2+}$  and substrate.

#### 6.4. Regio and stereoselective hydroxylations with metalloporphyrins without assistance of substrate recognition motifs

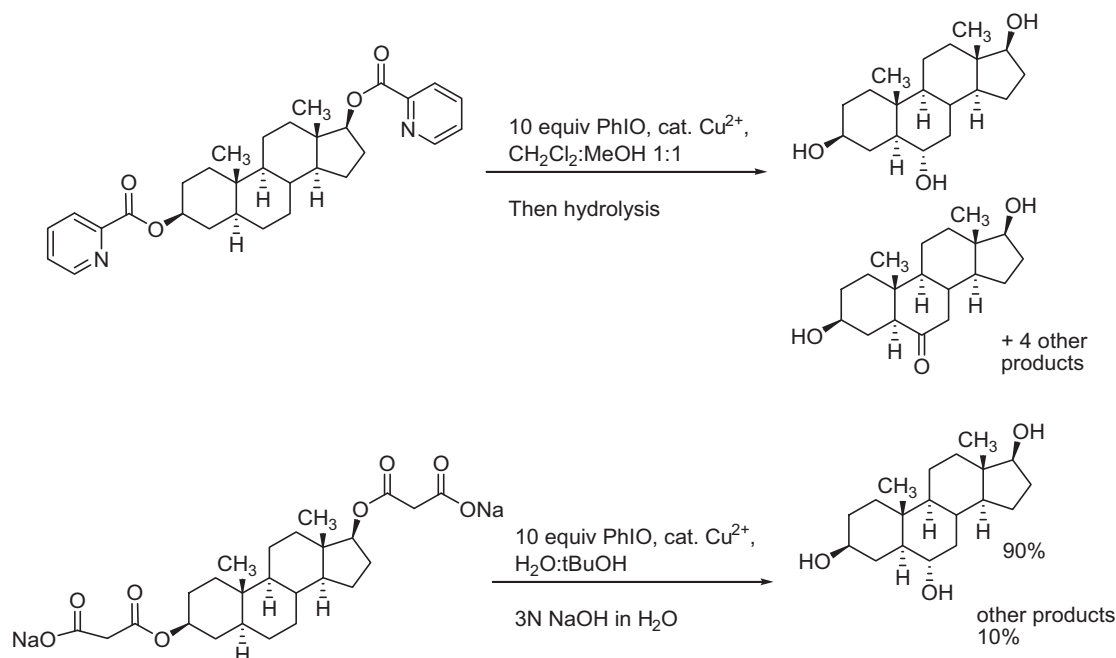
Highly selective allylic hydroxylation of triterpenes with an iron porphyrin was recently described by Konoiki et al. (Scheme 24) [136]. Low temperature reaction of MCPBA with  $[\text{Fe}(\text{TPFPP})\text{Cl}]$  afforded hydroxylated products in good to excellent yields (67–91%). Steric hindrance of the olefin functionality appears to be crucial in directing selectivity towards allylic C–H hydroxylation. Sterically non-hindered substrates are preferentially epoxidized by the same system.

Breslow et al. have described the regioselective oxidation of equilenin derivatives catalyzed by rhodium and manganese porphyrin complexes, using PhIO as oxidant (Scheme 25) [137]. Interesting differences in the regioselectivity of the oxidations was observed, depending on the nature of the porphyrin metal catalyst.  $[\text{Mn}(\text{TPFPP})\text{Cl}]$  oxidizes equilenin acetate (57% conversion) to a mixture of two products. Oxidation is regioselective affording pref-

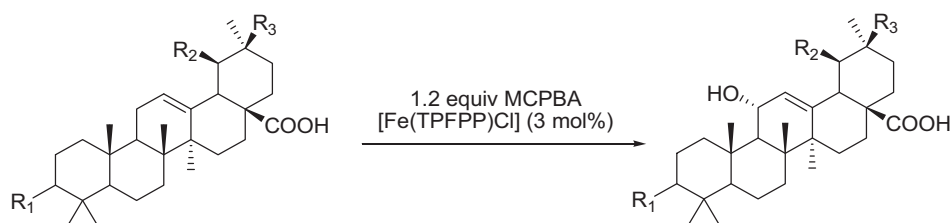
erentially C6-phenol (**E1**) in 74% yield based on conversion, and benzylic alcohol **E2** in 26% yield. No ketone arising from overoxidation of the latter product was obtained. Instead, when the rhodium catalyst  $[\text{Rh}(\text{TPFPP})\text{I}]$  was used, two different products (**E3** and **E4**), resulting from benzylic oxidation, were obtained in 57% and 43% relative yields (40% product conversion). Therefore, it appears that the putative  $\text{Rh}=\text{O}$  species preferentially hydroxylates the benzylic C–H bond, and overoxidizes the secondary benzylic alcohol, while the  $\text{Mn}=\text{O}$  species prefers to attack the aromatic ring.

#### 7. C–H Oxidations catalyzed by ruthenium and osmium porphyrins

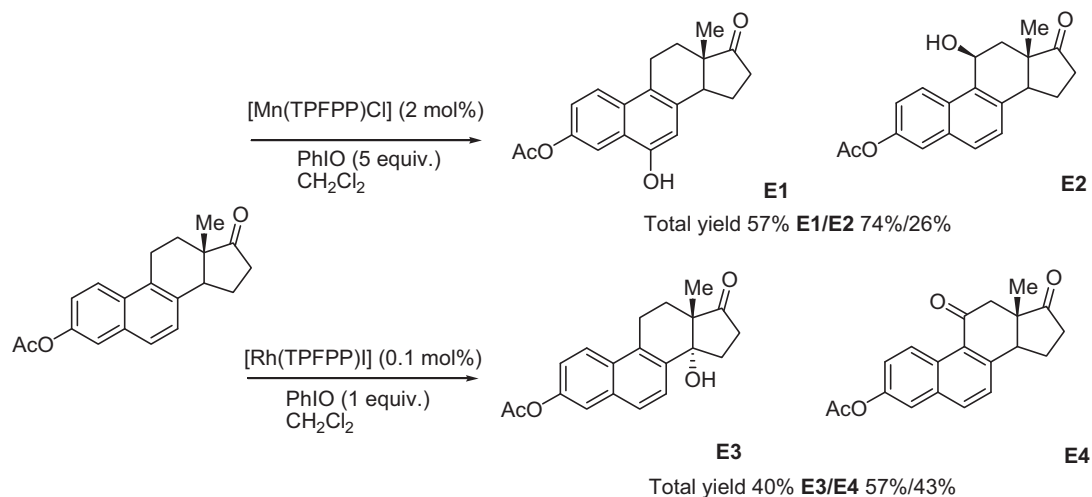
Besides Fe and Mn, Ru porphyrins have also proven to be particularly efficient C–H oxidation catalysts [12,138]. Hirobe et al. first described the use of Ru porphyrins in combination with 2,6-dichloropyridine-*N*-oxide ( $\text{Cl}_2\text{PyNO}$ ) as a very efficient system for the epoxidation of alkenes, and oxidation of alcohols and sulfides [139–141]. Alkanes are inert for this system. However, upon addi-



**Scheme 23.** Regio and stereoselective hydroxylation of steroid substrates using  $\text{Cu}^{2+}$  binding recognition motives (see Scheme 22 for catalyst structure). Top: Substrate contains acetylpyridine groups as  $\text{Cu}^{2+}$  binding units. Bottom: Substrate contains phosphonoacetyl groups as  $\text{Cu}^{2+}$  binding units.



**Scheme 24.** Selective allylic hydroxylation of triterpenes with  $[\text{Fe}(\text{TPFPP})\text{Cl}]$  and MCPBA.



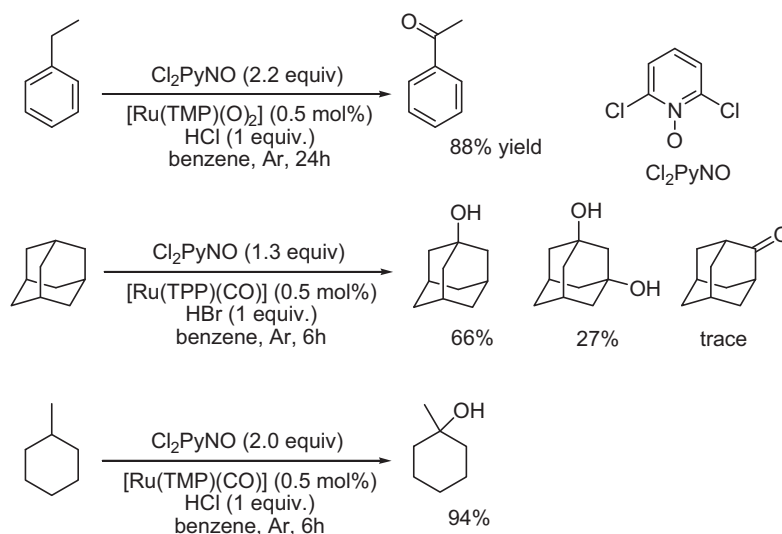
**Scheme 25.**  $[\text{Mn}(\text{TPFPP})\text{Cl}]$  and  $[\text{Rh}(\text{TPFPP})\text{I}]$  catalyzed oxidation of equilenin acetate.

tion of protic acids such as HBr, efficient hydroxylation of C–H bonds was accomplished (Scheme 26) [142]. Adamantane was very rapidly hydroxylated to 1-adamantanol and 1,3-adamantanediol, with TN reaching 100,000. Hydroxylation reactions are stereospecific, *cis*-decaline was primarily hydroxylated to 9-decalol, with no epimerization to the corresponding *trans*-isomeric alcohol [143].

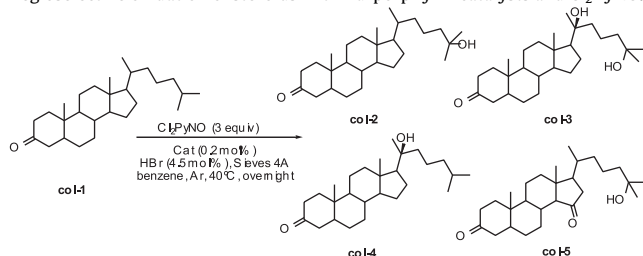
This system has been applied to the regio and stereoselective hydroxylation of steroids [144]. Hydroxylation reactions are stereospecific, retaining the chirality of the asymmetric centers. The regioselectivity of the oxidations was dependent on the steric bulk

of the ortho-substituents of the aromatic rings at the meso-position of the porphyrin catalysts, and on the electronic properties of the porphyrin (Table 4).

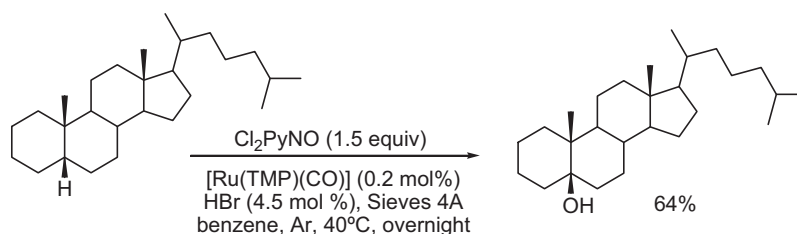
Remarkable good yields were obtained when 5 $\beta$ -steroids were oxidized to the corresponding 5 $\beta$ -hydroxy derivatives. For example, 5 $\beta$ -Cholestane was selectively hydroxylated to the corresponding 5 $\beta$ -hydroxy derivative in 64% yields (Scheme 27). Instead, under analogous conditions, 5 $\alpha$ -Cholestane was hydroxylated at the same 5 position in a more modest 14% yield. The authors suggest that different yields arise from the different steric encumbrance of the 5-H.



**Scheme 26.** Oxidation of ethylbenzene and alkanes with  $\text{Cl}_2\text{PyNO}$  and Ruthenium catalysts in the presence of HCl/HBr.

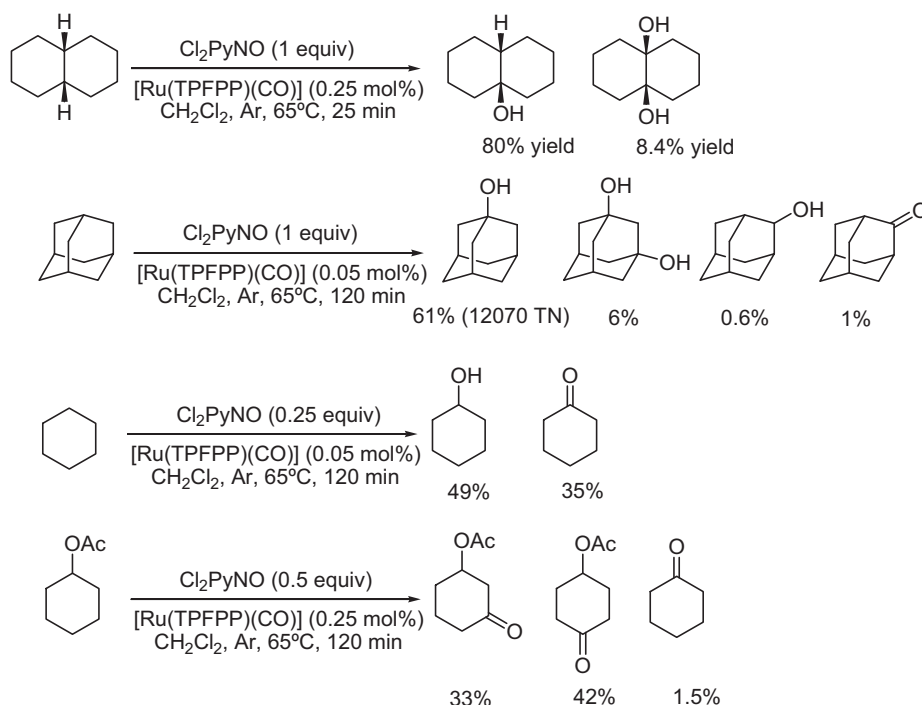
**Table 4**Regioselective oxidation of steroids with Ru-porphyrin catalysts and Cl<sub>2</sub>PyNO.

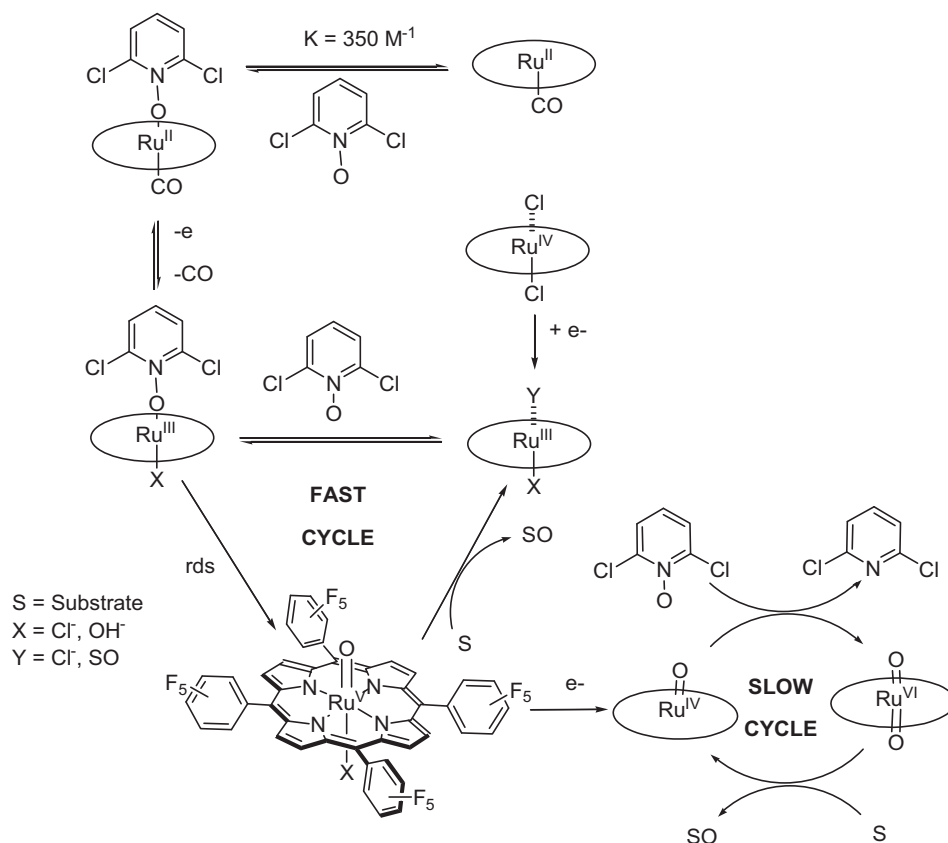
Entry	Catalyst	Col-2	Col-3	Col-4	Col-5
1	[Ru(TPP)(CO)]	11%	–	–	–
2	[Ru(TDCPP)(CO)]	25%	19%	6%	–
3	[Ru(TMP)(CO)]	26%	–	7%	12%

**Scheme 27.** Efficient hydroxylation of 5β-cholestane by [Ru(TMP)(CO)] and Cl<sub>2</sub>PyNO.

Groves et al. have reported that the perfluorinated porphyrin [Ru(TPFPP)(CO)] is a very efficient catalyst for the fast hydroxylation of hydrocarbons using 2,6-dichloropyridine *N*-oxide as oxidant, without the need of an acid (Scheme 28) [145,146]. Up to 14,800 TN were obtained in the hydroxylation of adamantane. Very interestingly, the oxidation is highly selective for the tertiary C–H bond. The normalized 3°/2° > 130 value is much higher than the analogous selectivity attained with Mn and Fe porphyrins (*vide infra*). On the other hand, reactions are stereospecific. The

hydroxylation of *cis*-decaline affords exclusively *cis*-9-decalol and *cis*-decaline-9,10-diol, and the oxidation of *trans*-decaline affords the corresponding *trans*-9-decalol. The oxidation of cyclohexyl acetate yields 3- and 4-acetoxycyclohexanone in 75% combined yield, based on oxidant consumed (0.5 equiv. with respect to substrate). No oxidation at position C-2 and only trace amounts of cyclohexanone were observed. Acetyl group provides thus protection against oxidation of C–H bonds in the α and β positions with respect to the acetate group. Oxidation of dibutyl ether

**Scheme 28.** Catalytic oxidation of C–H bonds with [Ru(TPFPP)(CO)] and Cl<sub>2</sub>PyNO.



**Scheme 29.** Mechanistic scheme for [Ru(TPFPP)(CO)] catalyzed oxidations with Cl<sub>2</sub>PyNO.

afforded 1-butanol and butyraldehyde in 80 and 92% yields, respectively, with respect to the oxidant (0.1 equiv. with respect to substrate).

Spectroscopic monitoring of the reactions indicate that [Ru<sup>IV</sup>(TPFPP)Cl<sub>2</sub>] and *trans*-dioxo-Ru complex [Ru<sup>VI</sup>(TPFPP)(O)<sub>2</sub>] are formed under catalytic conditions, but kinetic analyses show that the reaction of the substrate with the latter, albeit possible, is slow, incompatible with the fast reaction rates observed under catalytic conditions. Kinetic analyses showed induction periods and catalyst activation could be accomplished by reaction of [Ru<sup>IV</sup>(TPFPP)Cl<sub>2</sub>] with Zn amalgam. EPR analyses of this reaction, in the presence of EtOH evidences a rhombic set of signals,  $g = 2.53, 2.12$  and  $1.89$  characteristic of a  $S = \frac{1}{2}$  Ru<sup>III</sup> species. The sum of all these experimental evidences strongly suggests that a Ru<sup>III</sup>/Ru<sup>V</sup> cycle is responsible for the fast hydroxylation reactivity (Scheme 29). A highly electrophilic Ru<sup>V</sup>=O species is proposed to be responsible for the fast C–H oxidation activity via a rebound-type mechanism. Consistent with this proposal, <sup>18</sup>O is incorporated into oxidized products when reactions are performed in the presence of H<sub>2</sub><sup>18</sup>O, an observation that strongly supports the implication of a Ru<sup>V</sup>=O species that undergo water exchange via an oxo–hydroxo tautomerism [100]. A Hammett analysis of the relative reaction rates for the hydroxylation of *p*-substituted toluenes afforded an extraordinarily negative  $\rho^+ = -2.0$ , indicating that the Ru–oxo species are highly electrophilic. The P450 like mechanistic proposal is also consistent with the high KIEs = 4.8 measured in the intermolecular oxidation of equimolar mixtures of adamantane and *d*<sub>16</sub>-adamantane, and the stereospecificity of the reaction. However, despite of the KIE, the oxidation of adamantane displayed virtually the same reaction rate as the oxidation of its deuterated analogue, when analyzed in separate reaction experiments. That indicates that the rate determining step of the reactions is precedent to the C–H oxidation reaction.

Ru-porphyrin catalyst [Ru(TMP)Cl<sub>2</sub>] in combination with Cl<sub>2</sub>PyNO has been employed in the oxidation of amides. *N*-acyl cyclic amides were converted to the corresponding *N*-acylamino acids via oxidative C–N bond cleavage (Table 5) [147]. This system allows for the direct single-step oxidative conversion of *N*-acyl-L-proline derivatives to *N*-acyl-L-glutamates, which make this oxidation system useful in peptide chemistry. Lactams could be also effectively subjected to this oxidation.

Intramolecular kinetic isotope effect estimated in the oxidation of *N*-benzoyl[2,2-*d*<sub>2</sub>]pyrrolidine (Scheme 30) was  $9.8 \pm 0.2$  strongly suggesting that the rate determining step of the reaction involves H-atom abstraction.

The transformation was most likely initiated by hydroxylation at the carbon atom adjacent to the amine group, forming a hydroxylated amide that could be spectroscopically detected by NMR (Scheme 31).

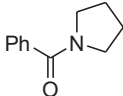
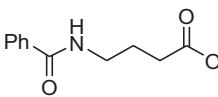
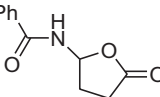
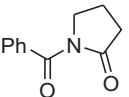
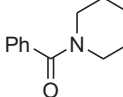
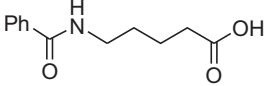
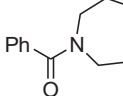
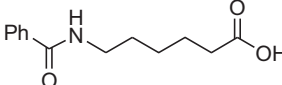
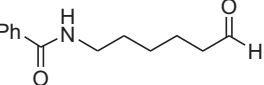
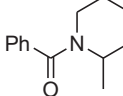
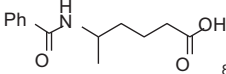
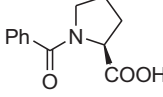
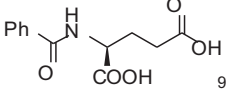
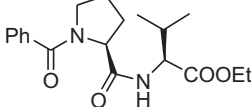
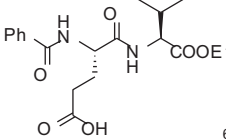
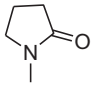
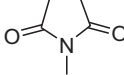
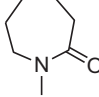
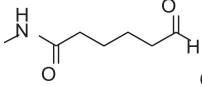
Oxidation of complex molecules could be also accomplished with ruthenium porphyrins. Che et al. have described that ketosteroids can be selectively oxidized in good yields to the corresponding diketosteroids by using [Ru(TDCPP)Cl<sub>2</sub>] as catalyst and Cl<sub>2</sub>PyNO as oxidant (Scheme 32). No epoxidation products were observed and turnover numbers over 900 were reached [148].

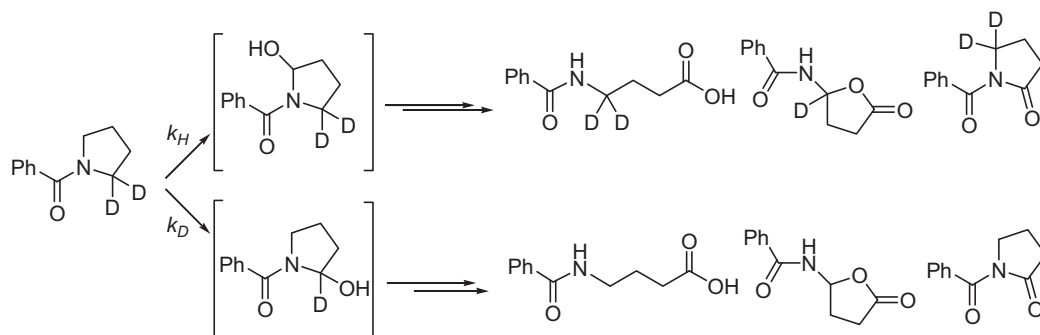
Finally, Iida and co-workers have shown that the combination of TBHP and [Os(TMP)(CO)] allows the single-step selective functionalization of complex organic molecules of biological relevance such as steroids [149], bile acids [150] and terpenoids [151].

## 8. Enantioselective C–H oxidations

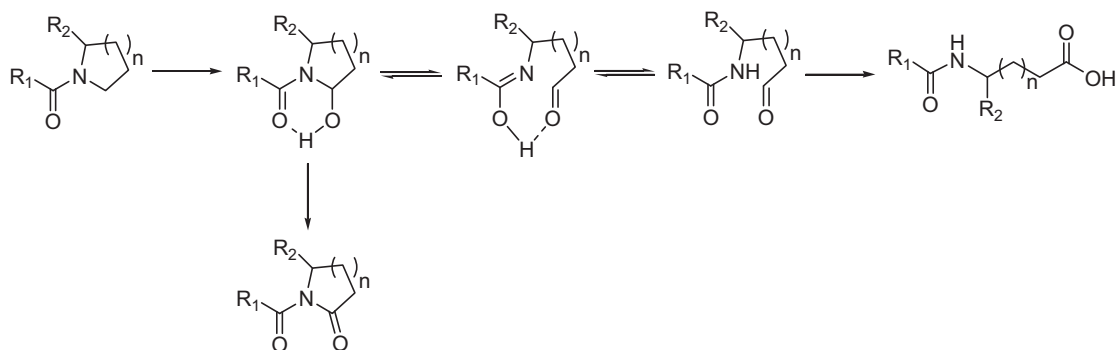
Porphyrin metalocatalysts constitute one of the very unique examples for which enantioselective C–H hydroxylation reactions have been described. Groves et al. reported vaulted binaphthyl iron or manganese porphyrins as enantioselective hydroxylation cata-

**Table 5**Catalytic oxidation of amides with [Ru(TMP)Cl<sub>2</sub>] and Cl<sub>2</sub>PyNO.<sup>a</sup>

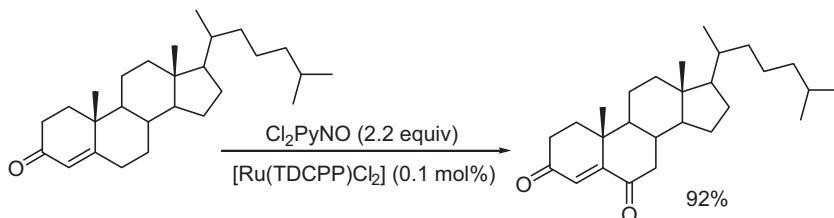
Substrate	Products, Isolated yield (%) <sup>b</sup>
	 66%  11%  4.6%
	 51%
	 41%  30%
	 89%
	 91%
	 63%
	 91% <sup>c</sup>
	 65% <sup>c,d</sup>

<sup>a</sup> Experimental conditions: substrate (0.16 M), [Ru(TMP)Cl<sub>2</sub>] (0.6 mol%), Cl<sub>2</sub>PyNO (0.32–0.40 M) stirred in benzene at 40 °C under Ar overnight.<sup>b</sup> Isolated yields based on substrate used.<sup>c</sup> Reaction took 2 days.<sup>d</sup> NMR yield.**Scheme 30.** Schematic diagram of the products formed in the oxidation of *N*-benzoyl[2,2-*d*<sub>2</sub>]pyrrolidine and *N*-benzoylpyrrolidine catalyzed by [Ru(TMP)Cl<sub>2</sub>], during KIE measurements.

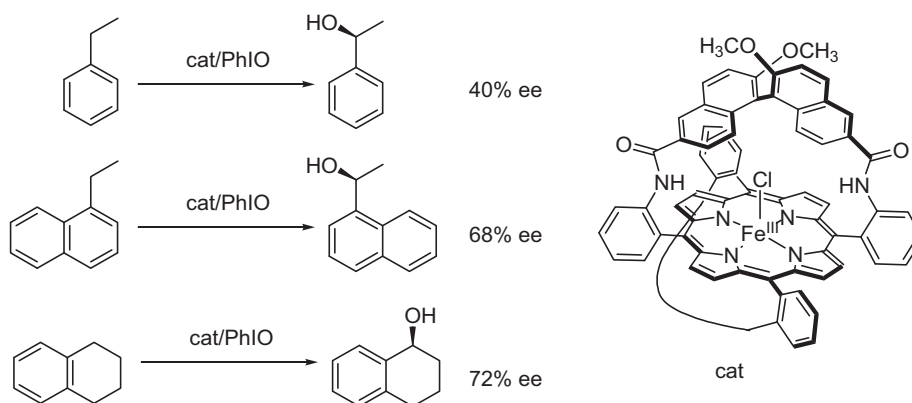




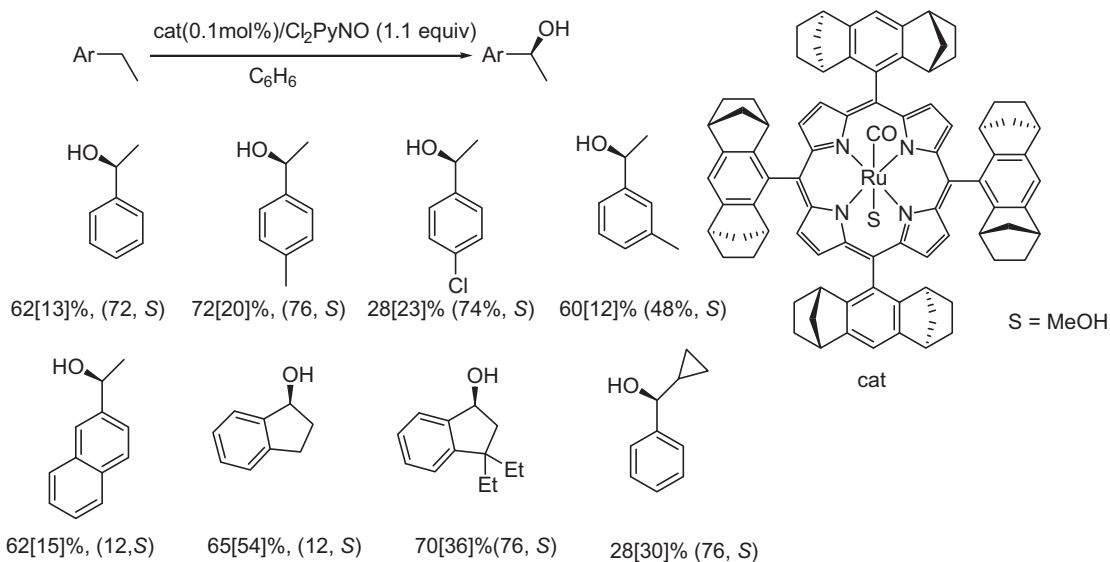
**Scheme 31.** Mechanistic diagram for the oxidation of amides with Ru-porphyrin catalysts.



**Scheme 32.** Efficient C–H oxidation of ketosteroids by [Ru(TDCPP)Cl<sub>2</sub>] and Cl<sub>2</sub>PyNO.



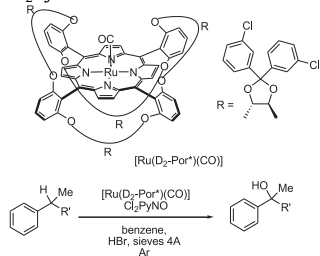
**Scheme 33.** Asymmetric hydroxylation of C–H bonds mediated by vaulted iron-binaphthyl porphyrins.



**Scheme 34.** Asymmetric hydroxylation of benzylic C–H bonds with Cl<sub>2</sub>PyNO mediated by [Ru<sup>II</sup>(D<sub>4</sub>-Por\*)(CO)(MeOH)] porphyrin. For each substrate, the bottom numbers indicate alcohol product yield with respect to substrate conversion [substrate conversion] (%ee, chirality).

**Table 6**

Asymmetric hydroxylation of 3° C–H bonds with  $d_2$ -symmetric porphyrins and  $\text{Cl}_2\text{PyNO}$ .



R'	Temp (°C)	Ee (%)	Yield (%)	TON
Bu	25	16	41	103
Et	25	27	54	135
Et	10	38	23	58

0.4  $\mu\text{mol}$  catalyst, 100  $\mu\text{mol}$  oxidant, 1 mmol alkane, 15  $\mu\text{l}$  48% HBr, 50 mg molecular sieves (4 Å) in 1 mL benzene under Ar.

lysts using PhIO as oxidant (Scheme 33) [76,152]. Alcohol yields, based on oxidant, ranged from 28 to 47%. Ee's up to 72% for the specific case of tetrahydronaphthalene were obtained.

Enantioselective hydroxylation of benzylic C–H bonds has also been accomplished with the chiral porphyrin [153] ruthenium catalyst  $[\text{Ru}(\text{D}_4\text{-Por}^*)(\text{CO})(\text{MeOH})]$  (Scheme 34) using  $\text{Cl}_2\text{PyNO}$  as oxidant. The system affords modest to good alcohol yields (28–90%, substrate conversions from 5 to 54%) and up to 76% ee [154–156].

Moderate ee's have been obtained in the asymmetric hydroxylation of tertiary C–H bonds of alkanes by using chiral  $\text{D}_2$  symmetric ruthenium metalloporphyrins as catalysts and  $\text{Cl}_2\text{PyNO}$  as oxidant (Table 6) [157]. Kinetic resolution of 2-phenylbutane was also performed with this system affording 8% enantiomerically enriched substrate and 18% ee tertiary alcohol.

## 9. Summary and future prospects

The unique ability of metalloporphyrins to catalyze the oxidation of C–H bonds with high selectivity has drawn major research interest during the last two decades. Very much has been advanced in the understanding of the fundamental details by which C–H bonds are hydroxylated by porphyrins, and the general mechanistic frame emerged from these studies has become a paradigm to understand C–H oxidation by virtually any metal–oxo species. On the other hand, in a moment where late stage alkane C–H functionalization reactions are at the forefront of the quest for novel, more straight and efficient synthetic strategies towards complex organic molecules, the selectivity and efficiency offered by metalloporphyrin catalysts are called to play a major role in the development of these technologies.

## Acknowledgements

Financial support for this work was provided by MEC-Spain (Project CTQ2009-08464), Generalitat de Catalunya (2009SGR637), and European Research Council for project ERC-2009-StG-239910. M.C. acknowledges an ICREA-Academia Award. Anna Company, Laura Gomez and Dr Julio Lloret are acknowledged by a critical reading of the manuscript. The author also thanks reviewers for helpful critical comments.

## References

- G. Dyker, Handbook of C–H Transformation, Wiley-VCH, Weinheim, 2005.
- G.A. Olah, Á. Molnár, Hydrocarbon Chemistry, 2nd ed., Wiley, New York, 2003.
- A.E. Shilov, G.B. Shul'pin, Activation and Catalytic Reactions of Saturated Hydrocarbons in the Presence of Metal Complexes, Springer-Verlag, Boston, 2000.
- R.A. Sheldon, J.A. Kochi, Metal-Catalyzed Oxidations of Organic Compounds, Academic Press, New York, 1981.
- J.A. Labinger, J.E. Bercaw, Nature 417 (2002) 507.
- K. Godula, D. Sames, Science 312 (2006) 67.
- K. Chen, P.S. Baran, Nature 459 (2009) 824.
- C.-M. Che, V.K.-Y. Lo, C.-Y. Zhou, J.-S. Huang, Chem. Soc. Rev. 40 (2011) 1950.
- J.M. Mayer, in: B. Meunier (Ed.), Biomimetic Oxidations Catalyzed by Transition Metal Complexes, Imperial College Press, London, 2000, p. 1.
- H. Lu, P. Zhang, Chem. Soc. Rev. 40 (2011) 1899.
- W. Nam, Acc. Chem. Res. 40 (2007) 522.
- J.T. Groves, Models, in: P.R. Ortiz de Montellano (Ed.), Cytochrome P450: Structure, Mechanism and Biochemistry, 3rd ed., Kluwer Academic/Plenum Publishers, New York, 2005, p. 1.
- F. Montanari, L. Casella, Metalloporphyrins Catalyzed Oxidations, Springer-Verlag, New York, 1994.
- D. Mansuy, Coord. Chem. Rev. 125 (1993) 129.
- B. Meunier, Chem. Rev. 92 (1992) 1411.
- B. Meunier, S.P. de Visser, S. Shaik, Chem. Rev. 104 (2004) 3947.
- P.R. Ortiz de Montellano, Cytochrome P450: Structure, Mechanism and Biochemistry, 3rd ed., Kluwer Academic/Plenum Publishers, New York, 2005.
- P.R. Ortiz de Montellano, Chem. Rev. 110 (2010) 932.
- M. Sono, M.P. Roach, E.D. Coulter, J.H. Dawson, Chem. Rev. 96 (1996) 2841.
- I. Schlichting, J. Berendzen, K. Chu, A.M. Stock, S.A. Maves, D.E. Benson, R.M. Sweet, D. Ringe, G.A. Petsko, S.G. Sligar, Science 287 (2000) 1615.
- B. Meunier, J. Bernadou, Struct. Bond. 97 (2000) 1.
- J.B. van Beilen, E.G. Funhoff, Curr. Opin. Biotechnol. 16 (2005) 308.
- T.L. Poulos, Curr. Biol. (1995) 767.
- T.L. Poulos, B.C. Finzel, A.J. Howard, J. Mol. Biol. 195 (1987) 687.
- C.K. Chang, M.-S. Kuo, J. Am. Chem. Soc. 101 (1979) 3413.
- J.T. Groves, T.E. Nemo, R.S. Myers, J. Am. Chem. Soc. 101 (1979) 1032.
- J.T. Groves, T.E. Nemo, J. Am. Chem. Soc. 105 (1983) 6243.
- C.K. Chang, F. Ebina, J. Chem. Soc. Chem. Commun. (1981) 778.
- J.T. Groves, T.E. Nemo, J. Am. Chem. Soc. 115 (1983) 5786.
- O. Bortolini, B. Meunier, J. Chem. Soc. Chem. Commun. (1983) 1364.
- P.S. Traylor, D. Dolphin, T.G. Traylor, J. Chem. Soc. Chem. Commun. (1984) 279.
- B.d. Poorter, B. Meunier, Tetrahedron Lett. 25 (1984) 1895.
- D. Dolphin, T.G. Traylor, L.Y. Xie, Acc. Chem. Res. 30 (1997) 251.
- A. Agarwala, D. Bandyopadhyay, Chem. Commun. (2006) 4823.
- T.G. Traylor, S. Tsuchiya, Inorg. Chem. 26 (1987) 1338.
- T. Wijesekera, A. Matsumoto, D. Dolphin, D. Lexa, Angew. Chem. Int. Ed. 29 (1990) 1028.
- P. Hoffmann, G. Labat, A. Robert, B. Meunier, Tetrahedron Lett. 31 (1990) 1991.
- P. Hoffmann, A. Robert, B. Meunier, Bull. Soc. Chim. Fr. 129 (1992) 85.
- S. Tsuchiya, M. Seno, Chem. Lett. 18 (1989) 263.
- M.W. Grinstaff, M.G. Hill, J.A. Labinger, H.B. Gray, Science 264 (1994) 1311.
- J.-F. Bartoli, K. Le Barch, M. Palacio, P. Battioni, D. Mansuy, Chem. Commun. (2001) 1718.
- S.R. Bell, J.T. Groves, J. Am. Chem. Soc. 131 (2009) 9640.
- W. Nam, Y.O. Ryu, W.J. Song, J. Biol. Inorg. Chem. 9 (2004) 654.
- J. Rittle, M.T. Green, Science 330 (2010) 933.
- A.-R. Han, Y.J. Jeong, Y.L. Kang, Jung Yoon, M.S. Seo, W. Nam, Chem. Commun. (2008) 1076.
- J.T. Groves, J. Inorg. Biochem. 100 (2006) 434.
- P.R. Ortiz de Montellano, J.J. De Voss, Nat. Prod. Rep. 19 (2002) 477.
- J.C. Schoneboom, H. Lin, N. Reuter, W. Thiel, S. Cohen, F. Ogliaro, S. Shaik, J. Am. Chem. Soc. 124 (2002) 8142.
- F.O. Ogliaro, S.R. de Visser, S. Cohen, J. Kaneti, S. Shaik, ChemBiochem 2 (2001) 848.
- X. Sheng, H. Zhang, S.-C. Im, J.H. Horner, L. Waskell, P.F. Hollenberg, M. Newcomb, J. Am. Chem. Soc. 131 (2009) 2971.
- Q. Wang, X. Sheng, J.H. Horner, M. Newcomb, J. Am. Chem. Soc. 131 (2009) 10629.
- X. Sheng, J.H. Horner, M. Newcomb, J. Am. Chem. Soc. 130 (2008) 13310.
- M. Newcomb, R. Zhang, R.E.P. Chandrasena, J.A. Halgrimson, J.H. Horner, T.M. Makris, S.G. Sligar, J. Am. Chem. Soc. 128 (2006) 4580.
- Z. Pan, Q. Wang, X. Sheng, J.H. Horner, M. Newcomb, J. Am. Chem. Soc. 131 (2009) 2621.
- Y.J. Jeong, Y. Kang, A.-R. Han, Y.-M. Lee, H. Kotani, S. Fukuzumi, W. Nam, Angew. Chem. Int. Ed. 47 (2008) 7321.
- W. Nam, S.E. Park, I.K. Lim, M.H. Lim, J.K. Hong, J. Kim, J. Am. Chem. Soc. 125 (2003) 14674.
- J.T. Groves, G.A. McCluskey, R.E. White, M.J. Coon, Biochem. Biophys. Res. Commun. 81 (1978) 154.
- J.T. Groves, G.A. McCluskey, J. Am. Chem. Soc. 98 (1976) 859.
- M.H. Gelb, D.C. Heimbrook, P. Malkonen, S.G. Sligar, Biochemistry 21 (1982) 370.
- J.T. Groves, D.V. Subramanian, J. Am. Chem. Soc. 106 (1984) 2177.
- T.G. Traylor, F. Xu, J. Am. Chem. Soc. 110 (1988) 1953.
- A. Sorokin, A. Robert, B. Meunier, J. Am. Chem. Soc. 115 (1993) 7293.
- Z. Pan, J.H. Horner, M. Newcomb, J. Am. Chem. Soc. 130 (2008) 7776.
- P.R. Ortiz de Montellano, R.A. Stearns, J. Am. Chem. Soc. 109 (1987) 3415.

- [65] K. Auclair, Z.B. Hu, D.M. Little, P.R. Ortiz de Montellano, J.T. Groves, *J. Am. Chem. Soc.* 124 (2002) 6020.
- [66] M. Newcomb, P.H. Toy, *Acc. Chem. Res.* 33 (2000) 449.
- [67] Y. Jiang, X. He, P.R. Ortiz de Montellano, *Biochemistry* 45 (2006) 533.
- [68] X. He, P.R. Ortiz de Montellano, *J. Biol. Chem.* 279 (2004) 39479.
- [69] M. Newcomb, R. Shen, Y. Lu, M.J. Coon, P.F. Hollenberg, D.A. Kopp, S.J. Lippard, *J. Am. Chem. Soc.* 124 (2002) 6879.
- [70] V.W. Bowry, K.U. Ingold, *J. Am. Chem. Soc.* 113 (1991) 5699.
- [71] P.H. Toy, M. Newcomb, P.F. Hollenberg, *J. Am. Chem. Soc.* 120 (1998) 7719.
- [72] J.K. Atkinson, K.U. Ingold, *Biochemistry* 32 (1993) 9209.
- [73] M. Newcomb, M.-H.L. Tadic-Biadatti, D.A. Putt, P.F. Hollenberg, *J. Am. Chem. Soc.* 117 (1995) 3312.
- [74] M. Newcomb, M.-H.L. Tadic-Biadatti, D.L. Chestney, E.S. Roberts, P.F. Hollenberg, *J. Am. Chem. Soc.* 117 (1995) 12085.
- [75] J.K. Atkinson, P.F. Hollenberg, K.U. Ingold, C.C. Johnson, M.-H. LeTadic, M. Newcomb, D.A. Putt, *Biochemistry* 33 (1994) 10630.
- [76] J.T. Groves, P. Viski, *J. Am. Chem. Soc.* 111 (1989) 8537.
- [77] J.L. McLain, J. Lee, J.T. Groves, in: B. Meunier (Ed.), *Biomimetic Oxidations Catalyzed by Transition Metal Complexes*, Imperial College Press, London, 2000, p. 91.
- [78] M. Newcomb, R. Shen, S.-Y. Choi, P.H. Toy, P.F. Hollenberg, A.D.N. Vaz, M.J. Coon, *J. Am. Chem. Soc.* 122 (2000) 2677.
- [79] M. Newcomb, D.L. Chestney, *J. Am. Chem. Soc.* 116 (1994) 9753.
- [80] R.D. Bach, O. Dimitrenko, *J. Am. Chem. Soc.* 128 (2006) 1474.
- [81] S. Shaik, S. Cohen, Y. Wang, H. Chen, D. Kumar, W. Thiel, *Chem. Rev.* 110 (2010) 949.
- [82] S. Shaik, H. Hirao, D. Kumar, *Acc. Chem. Res.* 40 (2007) 532.
- [83] S. Shaik, D. Kumar, S.P. de Visser, A. Altun, W. Thiel, *Chem. Rev.* 105 (2005) 2279.
- [84] F. Ogliaro, N. Harris, S. Cohen, M. Filatov, S.P. de Visser, S. Shaik, *J. Am. Chem. Soc.* 122 (2000) 8977.
- [85] S. Shaik, M. Filatov, D. Schröder, H. Schwarz, *Chem. Eur. J.* 4 (1998) 193.
- [86] S. Shaik, S. Cohen, S.P. de Visser, P.K. Sharma, D. Kumar, S. Kozuch, F. Ogliaro, D. Danovich, *Eur. J. Inorg. Chem.* 2 (2004) 207.
- [87] F. Ogliaro, S. Cohen, Shimrit, de Visser, P. Samuël, Shaik, Sason, *J. Am. Chem. Soc.* 122 (2000) 12892.
- [88] P.K. Sharma, S.P. de Visser, S. Shaik, *J. Am. Chem. Soc.* 125 (2003) 8698.
- [89] F. Ogliaro, S.P. de Visser, S. Cohen, P.K. Sharma, S. Shaik, *J. Am. Chem. Soc.* 124 (2002) 2806.
- [90] S.P. de Visser, F. Ogliaro, P.K. Sharma, S. Shaik, *Angew. Chem. Int. Ed.* 41 (2002) 1947.
- [91] F. Ogliaro, S.P. de Visser, J.T. Groves, S. Shaik, *Angew. Chem. Int. Ed.* 40 (2001) 2874.
- [92] N. Harris, S. Cohen, M. Filatov, F. Ogliaro, S. Shaik, *Angew. Chem. Int. Ed.* 39 (2000) 2003.
- [93] N. Suzuki, T. Higuchi, T. Nagano, *J. Am. Chem. Soc.* 124 (2002) 9622.
- [94] W. Nam, M.H. Lim, S.K. Moon, C. Kim, *J. Am. Chem. Soc.* 122 (2000) 10805.
- [95] J.P. Collman, A.S. Chien, T.A. Eberspacher, J.I. Brauman, *J. Am. Chem. Soc.* 122 (2000) 11098.
- [96] J.P. Collman, A.S. Chien, T.A. Eberspacher, J.I. Brauman, *J. Am. Chem. Soc.* 120 (1998) 425.
- [97] K.-B. Cho, Y. Moreau, D. Kumar, D.A. Rock, J.P. Jones, S. Shaik, *Chem. Eur. J.* 13 (2007) 4103.
- [98] W.J. Song, Y.J. Sun, S.K. Choi, W. Nam, *Chem. Eur. J.* 12 (2006) 130.
- [99] W. Nam, S.K. Choi, M.H. Lim, J.-U. Rohde, I. Kim, J. Kim, C. Kim, L. Que Jr., *Angew. Chem. Int. Ed.* 42 (2003) 109.
- [100] J. Bernadou, B. Meunier, *Chem. Commun.* (1998) 2167.
- [101] K.A. Lee, W. Nam, *J. Am. Chem. Soc.* 119 (1997) 1916.
- [102] Y. Kang, H. Chen, Y.J. Jeong, W. Lai, E.H. Bae, S. Shaik, W. Nam, *Chem. Eur. J.* 15 (2009) 10039.
- [103] S.P. de Visser, L. Tahsini, W. Nam, *Chem. Eur. J.* 15 (2009) 5577.
- [104] W. Nam, M.H. Lim, S.-Y. Oh, J.H. Lee, H.J. Lee, S.K. Woo, C. Kim, W. Shin, *Angew. Chem. Int. Ed.* 39 (2000) 3646.
- [105] T. Kamachi, T. Kouno, W. Nam, K. Yoshizawa, *J. Inorg. Biochem.* 100 (2006) 751.
- [106] R. Zhang, M. Newcomb, *Acc. Chem. Res.* 41 (2008) 468.
- [107] Z. Pan, R. Zhang, L.W.-M. Fung, M. Newcomb, *Inorg. Chem.* 46 (2007) 1517.
- [108] J. Bernadou, A.-S. Fabiano, A. Robert, B. Meunier, *J. Am. Chem. Soc.* 116 (1994) 9375.
- [109] J.T. Groves, R.C. Hausalter, M. Nakamura, T.E. Nemo, B.J. Evans, *J. Am. Chem. Soc.* 103 (1981) 2884.
- [110] W. Nam, J.S. Valentine, *J. Am. Chem. Soc.* 115 (1993) 1772.
- [111] C.L. Hill, B.C. Schardt, *J. Am. Chem. Soc.* 102 (1980) 6374.
- [112] J.T. Groves, W.J. Kruper Jr., R.C. Haushalter, *J. Am. Chem. Soc.* 102 (1980) 6375.
- [113] P. Battioni, J.P. Renaud, J.F. Bartoli, M. Reina-Artiles, M. Fort, D. Mansuy, *J. Am. Chem. Soc.* 110 (1988) 8462.
- [114] A. Thellend, P. Battioni, D. Mansuy, *J. Chem. Soc. Chem. Commun.* (1994) 1035.
- [115] C. Arunkumar, Y.-M. Lee, J.Y. Lee, S. Fukuzumi, W. Nam, *Chem. Eur. J.* 15 (2009) 11482.
- [116] W.J. Song, M.S. Seo, S.D. George, T. Ohta, R. Song, M.-J. Kang, T. Tosha, T. Kitagawa, E.I. Solomon, W. Nam, *J. Am. Chem. Soc.* 129 (2007) 1268.
- [117] N. Jin, M. Ibrahim, T.G. Spiro, J.T. Groves, *J. Am. Chem. Soc.* 129 (2007) 12416.
- [118] W. Nam, I. Kim, M.H. Lim, H.J. Choi, J.S. Lee, H.G. Jang, *Chem. Eur. J.* 8 (2002) 2067.
- [119] N. Jin, J.T. Groves, *J. Am. Chem. Soc.* 121 (1999) 2923.
- [120] J.T. Groves, J. Lee, S.S. Marla, *J. Am. Chem. Soc.* 119 (1997) 6269.
- [121] R. Zhang, J.H. Horner, M. Newcomb, *J. Am. Chem. Soc.* 127 (2005) 6573.
- [122] R. Zhang, M. Newcomb, *J. Am. Chem. Soc.* 125 (2003) 12418.
- [123] K.S. Suslick, F.V. Acholla, B.R. Cook, *J. Am. Chem. Soc.* 109 (1987) 2818.
- [124] J.Y. Lee, Y.-M. Lee, H. Kotani, W. Nam, S. Fukuzumi, *Chem. Commun.* (2009) 704.
- [125] J.F. Bartoli, O. Brigaud, P. Battioni, D. Mansuy, *J. Chem. Soc. Chem. Commun.* (1991) 440.
- [126] M.J. Nappa, C.A. Tolman, *Inorg. Chem.* 24 (1985) 4711.
- [127] B.R. Cook, T.J. Reinert, K.S. Suslick, *J. Am. Chem. Soc.* 108 (1986) 7281.
- [128] R. Breslow, Y. Huang, X. Zhang, J. Yang, *Proc. Natl. Acad. Sci. U.S.A.* 94 (1997) 11156.
- [129] R. Breslow, X. Zhang, Y. Huang, *J. Am. Chem. Soc.* 119 (1997) 4535.
- [130] J. Yang, R. Breslow, *Angew. Chem. Int. Ed.* 39 (2000) 2692.
- [131] J. Yang, B. Gabriele, S. Belvedere, Y. Huang, R. Breslow, *J. Org. Chem.* 67 (2002) 5057.
- [132] Z. Fang, R. Breslow, *Org. Lett.* 8 (2006) 251.
- [133] P.A. Grieco, T.L. Stuk, *J. Am. Chem. Soc.* 112 (1990) 7799.
- [134] M.D. Kaufman, P.A. Grieco, D.W. Bougie, *J. Am. Chem. Soc.* 115 (1993) 11648.
- [135] S. Belvedere, R. Breslow, *Bioorg. Chem.* 29 (2001) 321.
- [136] T. Konoike, Y. Araki, Y. Kanda, *Tetrahedron Lett.* 40 (1999) 6971.
- [137] J. Yang, R. Breslow, *Tetrahedron Lett.* 41 (2000) 8063.
- [138] S.-I. Murahashi, D. Zhang, *Chem. Soc. Rev.* 37 (2008) 1490.
- [139] H. Ohtake, T. Higuchi, M. Hirobe, *Tetrahedron Lett.* 33 (1992) 2521.
- [140] T. Higuchi, T. Ohtake, M. Hirobe, *Tetrahedron Lett.* 32 (1991) 7435.
- [141] T. Higuchi, H. Ohtake, M. Hirobe, *Tetrahedron Lett.* 30 (1989) 6545.
- [142] H. Ohtake, T. Higuchi, M. Hirobe, *J. Am. Chem. Soc.* 114 (1992) 10660.
- [143] H. Ohtake, T. Higuchi, M. Hirobe, *Heterocycles* 40 (1995) 867.
- [144] T. Shingaki, K. Miura, T. Higuchi, M. Hirobe, T. Nagano, *Chem. Commun.* (1997) 861.
- [145] J.T. Groves, M. Bonchio, T. Carofiglio, K. Shalyaev, *J. Am. Chem. Soc.* 118 (1996) 8961.
- [146] C. Wang, K.V. Shalyaev, M. Bonchio, T. Carofiglio, J.T. Groves, *Inorg. Chem.* 45 (2006) 4769.
- [147] R. Ito, N. Umezawa, T. Higuchi, *J. Am. Chem. Soc.* 127 (2005) 834.
- [148] J.L. Zhang, C.-M. Che, *Chem. Eur. J.* 11 (2005) 3899.
- [149] T. Iida, S. Ogawa, K. Hosoi, M. Makino, Y. Fujimoto, T. Goto, N. Mano, J. Goto, A.F. Hofmann, *J. Org. Chem.* 72 (2007) 823.
- [150] S. Ogawa, K. Hosoi, T. Iida, Y. Wakatsuki, M. Makino, Y. Fujimoto, A.F. Hofmann, *Eur. J. Org. Chem.* (2007) 3555.
- [151] S. Ogawa, Y. Wakatsuki, M. Makino, Y. Fujimoto, K. Yasukawa, T. Kikuchi, M. Ukiya, T. Akihisa, T. Iida, *Chem. Phys. Lipids* 163 (2010) 165.
- [152] J.T. Groves, P. Viski, *J. Org. Chem.* 55 (1990) 3628.
- [153] R.L. Halterman, S.T. Jan, H.L. Nimmons, D.J. Standlee, M.A. Khan, *Tetrahedron* 53 (1997) 11257.
- [154] R. Zhang, W.Y. Yu, T.S. Lai, C.-M. Che, *Chem. Commun.* (1999) 1791.
- [155] R. Zhang, W.-Y. Yu, C.-M. Che, *Tetrahedron Asymmetry* 16 (2005) 3520.
- [156] C.-M. Che, J.-S. Huang, *Chem. Commun.* (2009) 3996.
- [157] Z. Gross, S. Ini, *Org. Lett.* 1 (1999) 2077.